

Clonal analysis of *Salmonella*-specific effector T cells reveals serovar specific and cross-reactive T cell responses

Giorgio Napolitani¹, Prathiba Kurupati¹, Karen Wei Weng Teng², Malick M Gibani⁴, Margarida Rei¹, Anna Aulicino¹, Lorena Preciado-Llanes^{1,3}, Michael Thomas Wong², Etienne Becht², Lauren Howson¹, Paola de Haas¹, Mariolina Salio¹, Christoph J. Blohmke⁴, Lars Rønn Olsen⁵, David Miguel Susano Pinto⁶, Laura Scifo¹, Claire Jones⁴, Hazel Dobinson⁴, Danielle Campbell⁴, Helene B Juel⁴, Helena Thomaides-Brears⁴, Derek Pickard⁷, Dirk Bumann⁸, Stephen Baker⁹, Gordon Dougan⁷, Alison Simmons¹, Melita A. Gordon^{3,10}, Evan William Newell², Andrew J Pollard⁴, Vincenzo Cerundolo¹.

¹ MRC Human Immunology Unit, Weatherall Institute of Molecular Medicine, University of Oxford, UK;

² Singapore Immunology Network, Agency of Science, Technology and Research, Singapore;

³ Institute of Infection and Global Health, University of Liverpool, UK;

⁴ Oxford Vaccine Group, Department of Paediatrics, University of Oxford and the NIHR Oxford Biomedical Research Centre, Oxford, UK;

⁵ Department of Bio and Health Informatics, Technical University of Denmark, Copenhagen, DK;

⁶ Micron Oxford, Department of Biochemistry, University of Oxford

⁷ Wellcome Trust Sanger Institute, Cambridge, UK.

⁸ Biozentrum, University of Basel, CH.

⁹ Hospital for Tropical Diseases, Wellcome Trust Major Overseas Programme, Oxford University Clinical Research Unit, Ho Chi Minh City, Vietnam.

¹⁰ Malawi-Liverpool-Wellcome Trust Clinical Research Programme, Malawi.

Abstract

To tackle the complexity of cross-reactive and pathogen specific T cell responses against related *Salmonella* serovars, we used mass cytometry, unbiased single cell cloning, live fluorescent barcoding, and T cell receptor sequencing, to reconstruct the *Salmonella* specific repertoire of circulating effector CD4⁺ T cells, isolated from volunteers challenged with *Salmonella enterica* serovar Typhi (*S. Typhi*) or *Salmonella* Paratyphi A (*S. Paratyphi*).

We described the expansion of cross-reactive responses against distantly related *Salmonella* Serovars and of clonotypes recognizing immunodominant antigens uniquely expressed by *S. Typhi* or *S. Paratyphi*. In addition, single amino acid variations in two immunodominant proteins, CdtB and PhoN, lead to the accumulation of T cells not cross-reacting against the different serovars, demonstrating how minor sequence variations in a complex microorganism shape the pathogen specific T cell repertoire. Our results identify immune-dominant serovar specific and cross-reactive T cell antigens, which will help the design of T cell vaccination strategies against *Salmonella*.

Introduction

Dissecting the repertoire of antigen specific T cell responses to bacteria has been hampered by the relatively large number of proteins expressed by bacteria, and by the presence of cross-reactive T cell responses as a consequence of the large degree of sequence homology between related bacterial species.

Enteric fever (also known as typhoid fever) is responsible for over 20 million cases and 150,000 deaths annually ^{1, 2, 3} and is caused by *Salmonella enterica* serovar Typhi (*S. Typhi*) and *Salmonella enterica* serovar Paratyphi A (*S. Paratyphi A*), collectively referred to as typhoidal *Salmonella* serovars of the gastrointestinal pathogen *Salmonella enterica*. *S. Typhi* and *S. Paratyphi A* are human restricted, spread systemically in apparently uncompromised hosts, and cause life threatening infections ⁴. In comparison, non-typhoidal *Salmonella* serovars (NTS), such as *Salmonella* Typhimurium (*S. Typhimurium*) and *Salmonella* Enteritidis (*S. Enteritidis*), typically cause a localized gastrointestinal infection in immunocompetent hosts ⁵. *S. Typhi* and *Paratyphi A* share an estimated ~95% of their proteome and ~85% with *S. Typhimurium* ^{6, 7}.

The design of vaccination strategies capable of protecting against different serovars requires a better understanding of the impact of pathogen genetic variation/divergence on pathogen specific responses elicited during infection with the different *Salmonella* serovars, and the identification of serovar specific antigens and epitopes, which could guarantee appropriate coverage.

Both B and T cell responses are known to contribute to protection in mouse models of *Salmonella* infection and vaccination. While B cells can confer the first line of protection against mucosal invasion and systemic dissemination, T cells are needed for the efficient clearance of *Salmonella* ⁸. In particular, CD4⁺ T cells play a major protective role in mouse models of *S. Typhimurium* infection ⁹, with CD8⁺ T cells not essential for acquired immunity to this pathogen ¹⁰. Additionally, genome wide association studies have shown that expression of specific MHC class II alleles confer resistance to enteric fever, suggesting a protective function of CD4⁺ T cells in the control of *S. Typhi* and *S. Paratyphi A* infection in humans ¹¹.

Humans are the only known natural host of *S. Typhi* and *Paratyphi A*, and we have recently established a human infection model of enteric fever in healthy adult volunteers based on earlier challenge studies^{12, 13, 14}.

In this study, we aimed to characterize Salmonella specific CD4⁺ T cells based on their capacity to cross-react or not against distinct Salmonella serovars, and to identify antigens capable of mediating this cross-reactivity or lack thereof.

This requires: *i)* precise knowledge of the primary sequence of immunogenic proteins and pathogen's proteome; *ii)* samples collected at the peak of the immune response from infected individuals with no other concurrent infections; *iii)* accurate identification of effector T cells responding to immunization/infection; *iv)* the possibility to test individual T cells for their capacity of recognizing target cells infected with distinct bacteria.

In order to meet the first and second requirements, we used samples collected from volunteers experimentally challenged with *S. Typhi* and *Paratyphi A*. Next, we used mass cytometry to identify a population of effector of CD38⁺CCR7⁻IFN- γ ⁺ Mip-1 β ⁺ CD4⁺ T cell differentiating in the peripheral blood of volunteers with enteric fever, and finally we performed unbiased single T cell cloning to reconstruct *in-vitro* the antigen specific repertoire of this population of effector T cells.

Results

Phenotypic and functional characterization of CD4⁺ T cell responding to enteric fever.

In order to identify CD4⁺ effector T cells circulating during *Salmonella* infection, we utilized mass cytometry to perform deep phenotypic profiling of CD4⁺ T cells in frozen peripheral blood mononuclear cells (PBMCs) collected from human volunteers with a confirmed diagnosis of enteric fever, initially focusing upon experimental infection with live *S. Paratyphi A*.

PBMCs were collected and frozen at baseline (D0) and at multiple time points covering the different phases of infection: incubation (four days after challenge), enteric fever (2-4 days after diagnosis), resolution of infection (28 and 90 days after challenge) (Fig. 1a). Frozen PBMCs were thawed and either stained with a panel of metal conjugated antibodies directed against a wide range of phenotypic, proliferation and homing markers (Supplementary Table 1, Proliferation and Trafficking Panel), or stimulated with Phorbol 12-myristate 13-acetate (PMA) and Ionomycin, and stained with a second mass cytometry panel of antibodies capable of detecting the expression of different cytokines and activation markers (Supplementary Table 1, Function and Trafficking Panel).

First, we measured the frequency of CD4⁺ T cells expressing the intracellular marker of proliferation Ki67 (Supplementary Fig. 1a). At baseline, all volunteers showed a low, but detectable, frequency of Ki67⁺CD4⁺ T cells (median=0.52%, max=0.82%, min=0.17%, (Fig. 1b), which transiently increased in samples collected after diagnosis of enteric fever (median=1.51%, max=1.76%, min=0.94%), suggestive of an accumulation of proliferating T cells upon infection.

Next, we analysed the phenotype of Ki67⁺ T cells, and asked whether their proliferation was associated to the selective accumulation of a phenotypically distinct subset of effector T cells, or to an overall increase in T cell proliferation. Phenograph¹⁵ clustering of Ki67⁺ T cells detected in all different volunteers across the distinct phases of infection identified 20 distinct subsets (Fig. 1c). Samples collected after enteric fever diagnosis showed an increase in the proportion of cells within subset 19, which increased from a median of 4.1% of Ki67⁺ T cells (and of 0.02% of total CD4⁺ T cells) at time of challenge to a median of 36.2 % (0.47% of CD4⁺ T cells) at the peak of disease (Fig. 1d and Supplementary Fig. 1b,c). Subset 19 cells were characterized by elevated expression of the activation markers CD38 and ICOS, of CD127, of T_H1(CXCR3 and CCR5) and mucosal tissues (Integrin β 7 and CD49d) homing markers, and by a lower expression of skin and T_H2 homing markers such as CLA and CCR4, of the lymph-node homing marker CCR7 and of the survival factor BCL2 (Fig. 1e and Supplementary Fig. 1d).

Next, we noticed that cells within subset 19 cells were characterized by elevated expression of CD38 and low expression of CCR7 (Fig. 1e and Supplementary Fig. 2a). Three lines of evidence suggest that CD38⁺CCR7⁻ cells might recapitulate subset 19 within total CD4⁺ cells: 1) CD38⁺CCR7⁻ were rare at baseline and after resolution of infection, but their frequency increased after the onset of clinical symptoms and bacteremia (Fig. 1f-g), 2) although cluster 7, 8, 15 and 20 also contained CD38⁺CCR7⁻ T cells, their frequency accounted only for a minor proportion of Ki67⁺ T cells in enteric fever samples (Supplementary Fig. 2b); 3) only the frequency of Ki67⁺ contained within CD38⁺CCR7⁻ cells significantly increased after diagnosis (Supplementary Fig. 2c).

Multicolor flow cytometry on fresh whole blood samples confirmed the accumulation of CD38⁺CCR7⁻ T cells in volunteers who developed enteric fever upon challenge with *S. Typhi*

or *S. Paratyphi* A (Supplementary Fig. 3a,b), hence supporting the notion that CD38⁺CCR7⁻ T cells represent bona fide effector cells released during typhoidal *Salmonella* infection.

Functional characterization of CD4⁺CD38⁺CCR7⁻ T cells induced during enteric fever

To characterize the functional profile of CD4⁺ T cells responding to *Salmonella* infection, we used CCR7 and CD38 to identify effector T cells in PBMC stimulated with the polyclonal stimuli PMA and Ionomycin, and stained with the Function and Trafficking mass cytometry panel (Supplementary Table 1).

CD38⁺CCR7⁻ T cells were enriched in cells capable of producing IFN- γ , MIP-1 β and TNF, and expressing CD40L and CTLA4 (Fig. 2a-b). To understand whether CCR7⁻CD38⁺ effector T cells represent a functionally homogeneous subset of CD4⁺ T cells endowed with specific effector functions, we performed t-distributed stochastic neighbor embedding (tSNE) to map in a bidimensional plot the heterogeneity of antigen experienced CD45RA⁻ T cells based on their capacity to express different cytokines and functional markers (Fig. 2c). In contrast to the total pool of non-naive CD45RA⁻CD4⁺ T cells, a large proportion of CD38⁺CCR7⁻ T cells was concentrated in a small region of this bi-dimensional map enriched in cells capable of producing MIP1- β and IFN- γ (Fig. 2d-e).

This mass cytometry analysis revealed that *Salmonella* infection is associated with the release in peripheral blood of a functionally homogeneous population of IFN- γ Mip-1 β producing CD38⁺CCR7⁻CD4⁺ effector T cells, endowed with the capacity to migrate to mucosal tissues, potentially through the expression of the integrins CD49d and Integrin β 7 and to sites of T_H1 inflammatory responses, attracted by agonists of CCR5 and CXCR3.

Cloning of CD38⁺CCR7⁻ effector CD4⁺ T cells to characterize the repertoire of *Salmonella* specific T cells.

We next developed a single cell approach to dissect the antigen specific repertoire of effector CD38⁺CCR7⁻CD4⁺ T cells (Fig. 3), and determine the proportion of individual effector T cell responding to distinct serovars. CD38⁺CCR7⁻CD4⁺ T cells, isolated from volunteers after diagnosis of enteric fever were sorted as single cells, expanded *in vitro* in the presence of phytohemagglutinin (PHA) and IL-2 for at least 3 weeks, and tested for their capacity to recognize autologous EBV transformed lymphoblastoid cell lines (EBV-LCL) infected with live *Salmonella* (Fig. 3a). To minimize experimental variability when comparing different T cell clones and enable high throughput screening of T cell clone specificity, we developed a fluorescence cellular barcoding approach¹⁶ to perform short-term antigen specific stimulation of distinct T cell clones in a single tube (Fig. 3b and Supplementary Fig. 4). CD4⁺ T cell clones generated from a single volunteer were labelled with distinct dilutions of up to four different fluorescent dyes, pooled, and stimulated with autologous EBV-LCL pulsed with different *Salmonella* serovars, strains or antigens. Then, we used multicolor flow cytometry to discriminate T cell clones by their specific fluorescent barcoding, and IFN- γ intracellular cytokine staining to identify the pathogen specific T cell clones.

Libraries generated from CD38⁺CCR7⁻ T cells were enriched in T cell clones capable of producing IFN- γ in the presence of autologous EBV LCL infected with *S. Typhi* (Quailes, and Ty21a vaccine strain), as compared with CD38⁺CCR7⁻ T cells, (Fig. 3c,d), consistent with the notion that CD38⁺CCR7⁻ circulating T cells during enteric fever are enriched in *Salmonella* specific CD4⁺ T cells.

Further analysis of libraries of CD38⁺CCR7⁻ T cell clones generated from 4 more volunteers challenged with *S. Typhi* (T3, T4, T5 and T6) and 2 with *S. Paratyphi A* (P1 and P2)

confirmed that CD38⁺CCR7⁻ T cells were enriched in clones specific for the pathogen used for the *in vivo* challenge (min=20%, max=86%) (Fig. 3e,f).

Next, T cell clones were compared for their capacity of recognizing target cells infected with the two typhoidal serovars *S. Typhi* and *S. Paratyphi A*, and with the non-typhoidal serovar *S. Typhimurium*. Between 35 and 71% of them were cross-reactive against autologous EBV-LCL infected with either *S. Typhi* (Ty21a, Quailles or BRD948 strains), *S. Paratyphi A* (NVGH308 strain) or *S. Typhimurium* (D25380, LT2 strains) (Fig. 4a,b-d). However, in each volunteer we identified T cell clones not cross-reactive against *S. Typhimurium*, but capable of recognizing autologous EBV-LCL infected with *S. Typhi*, *S. Paratyphi A* or both (Fig. 4a and e), indicating that the antigen specific repertoire of CD38⁺CCR7⁻ T cells developing in response to *S. Typhi* and *Paratyphi* infection was enriched in *Salmonella* specific T cells, and comprised both serovar specific and cross-reactive T cells.

HlyE and CdtB specific CD4⁺ T cells account for a large fraction of the typhoidal specific T cell clones.

The analysis of effector CD38⁺CCR7⁻ CD4⁺ T cell clones described above gave us the opportunity of reconstructing *in-vitro* the heterogeneity of the CD4⁺ T cell response, discriminating individual T cells based on their ability to cross-react or not with cells infected with distinct serovars. We reasoned that the same approach could be used to identify antigens capable of mediating this cross-reactivity or lack thereof, and determine the proportion of effector T cells recognizing these antigens within the total of the *Salmonella* specific T cells. Hemolysin E (HlyE) and cytolethal distending toxin B (CdtB), a component of typhoid toxin^{17, 18}, have been characterized as immunodominant B cell antigens¹⁹ expressed by the typhoidal serovars *S. Typhi* and *S. Paratyphi A*, but predominantly not by non-typhoidal

serovars^{20, 21}. We designed two peptide pools encompassing the entire protein sequences of HlyE and CdtB in *S. Typhi* and *S. Paratyphi A* and asked whether these might represent targets for the typhoid and paratyphoid specific fraction of CD38⁺CCR7⁻CD4⁺ T cell clones. We detected HlyE specific CD4⁺ T cell clones in 6 and CdtB specific CD4⁺ T cell clones in 5 out of the 8 volunteers analysed. As expected, T cell clones reactive against HlyE and CdtB were not capable of recognizing cells infected with *S. Typhimurium* (Fig. 5a,b) and, where present, CdtB specific T cell clones comprised from 9% to 40%, while HlyE specific T cell clones from 11% to 80% of the typhoidal specific T cell fraction (Fig. 5c). ELISPOT analysis on fresh PBMC confirmed an increased frequency of IFN- γ producing T cells specific for HlyE and CdtB in challenged volunteers compared with healthy controls, with a greater response in volunteers who developed enteric fever after challenge, compared with those who did not (Supplementary Fig. 5).

Furthermore, HlyE specific T cell clones differed in their capacity to respond to distinct typhoidal strains: recognizing cells infected with the live attenuated vaccine *S. Typhi* strain Ty21a more efficiently than cells infected with the challenge strains *S. Typhi* Quail and *S. Paratyphi A* NVGH308 (Fig. 5d,e), consistent with the observation that Ty21a has increased HlyE dependent hemolytic activity *in vitro*, as compared with other typhoidal strains²².

Salmonella specific CD4⁺ T cells recognize both constitutively expressed and inducible bacterial antigens.

The expression of CdtB, as well as that of several virulence factors involved in *Salmonella* pathogenesis, is induced only upon infection of target cells¹⁷ (Fig. 5f). Thus, we asked whether we could discriminate T cell clones recognizing antigens expressed only upon infection from those recognizing antigens constitutively expressed by the bacteria. To answer this question, we compared the capacity of different *Salmonella* specific CD4⁺ T cell clones

to recognize either autologous EBV-LCL pulsed with a lysate of a liquid culture of *S. Typhi* strain BRD948 or infected with live bacteria. A large number of *Salmonella* specific CD4⁺ T cell clones, including those specific for CdtB, were capable of recognizing only cells infected with live bacteria, suggesting that a significant proportion of the CD4⁺ T cell response against *Salmonella* targets antigens expressed only upon infection (Fig. 5g).

These results show how the antigen specific repertoire of *Salmonella* specific CD4⁺ T cells is shaped by the transcriptional plasticity of *Salmonella* and highlight the importance of characterizing pathogen specific T cell responses directed against antigen expressed in infected tissues.

Identification of CdtB specific CD4⁺ T cell clones non cross-reactive against *S. Typhi* and *S. Paratyphi A*.

The above data provide the first evidence that CdtB, a toxin involved in the pathogenic mechanisms of the typhoidal serovars, is a major T cell target of CD4⁺ T cell responses against typhoidal *Salmonella*. The role of CD4⁺ T cells in protection against intracellular bacteria such as *Salmonella* is largely dependent on their capacity to secrete cytokines capable of helping macrophages in controlling bacterial growth. Indeed, CdtB specific T cell clones were able to limit bacterial spread in vitro (Supplementary Fig. 6), suggesting that these T cell clones might be able to exert a similar role *in vivo*.

However, although CdtB is expressed by both typhoidal serovars, some of the isolated CdtB specific T cell clones failed to recognize cells infected with both bacteria. In particular, six of the CdtB specific T cell clones identified in volunteer T4 recognized autologous EBV-LCL infected with the *S. Typhi* strains (Fig. 6a), but not cells infected with *S. Paratyphi A*.

The 185aa CdtB protein sequence differs in only two aminoacids in *S. Typhi* compared to *S. Paratyphi A*: at position 110, with a Tyrosine in *S. Paratyphi A* and Histidine in *S. Typhi*

(H110Y); and at position 228, with a Serine in *S. Paratyphi* A and Glutamine in *S. Typhi* (S228Q) (Fig. 6b). Epitope mapping of CdtB specific T cell clones revealed that these recognized a region of the *S. Typhi* CdtB sequence spanning across the Histidine in position 110. However, while all CdtB specific cross-reactive clones were activated by CdtB peptides containing either Histidine (*S. Typhi* variant) or Tyrosine (*S. Paratyphi* A) at position 110, *S. Typhi* CdtB specific T cell clones were activated exclusively by CdtB peptides containing the *S. Typhi* Histidine variant (Fig. 6c).

A similar lack of cross-reactivity was also observed in a volunteer (P1) challenged with *S. Paratyphi* A (Fig. 6d-e), where two CdtB specific CD4⁺ T cell clones were characterized: the first (clone 99) recognized an epitope present within a conserved region of CdtB (25-45) and reacted to both *S. Paratyphi* A and *S. Typhi* infected cells; the second (clone 106) reacted only to *S. Paratyphi* A infected cells (Fig. 6e), recognized peptides spanning the region across position 110, but only those containing the *S. Paratyphi* A variant 110Y.

Using a panel of partially matched EBV-LCL, we demonstrated that the CdtB(105-125) specific T cell clones isolated from volunteers T4, T5 and P1 were HLA-DRB4 restricted. ELISPOT analysis on frozen PBMC collected before challenge and after resolution of infection showed that the increased frequency of CdtB specific IFN- γ producing T cells was more pronounced in HLA-DRB4⁺ compared to HLA-DRB4⁻ individuals (Supplementary Fig. 7a and b), suggesting that CdtB(105-125) might be a major determinant in the CdtB CD4 T cell response to typhoidal *Salmonella*.

The distinct specificity of CdtB(105-125) specific T cell clones against *S. Typhi* and *S. Paratyphi* A was confirmed by using HLA-DRB4 tetramers loaded with either the ST(110H) or the SP(110Y) CdtB peptide, demonstrating differential tetramer staining of cross-reactive, *Paratyphi* specific and *Typhi* specific CD4⁺ T cell clones (Fig. 6f). Furthermore, these tetramers were used to measure the *ex-vivo* frequency of CdtB 105-125 specific HLA-DRB4

restricted CD4⁺ T cells in frozen PBMC from HLA-DRB4⁺ volunteers collected before and after challenge with *S. Typhi* and *S. Paratyphi A*. The frequency of CD4⁺ T cells stained by either of the two HLA-DRB4 tetramers increased after challenge (Fig. 6g), but notably, volunteers challenged with *S. Typhi* showed an accumulation of effector T cells preferentially stained by the HLA-DRB4 tetramers loaded with the CdtB(105-125) ST110H peptide, while volunteers challenged with *S. Paratyphi A* showed a preferential accumulation of clones stained by the HLA-DRB4 tetramers loaded with the CdtB(105-125) ST110Y peptide (Fig. 6h,i).

These data show that a single amino acid difference in a shared immunodominant antigen can elicit divergent serovar specific non cross-reactive responses, and is a major target of T cells non-cross-reactive against the two typhoidal serovars.

Identification of antigens recognized by non-typhoidal *Salmonella* cross-reactive T cell clones.

The identification of T cell antigens shared across different typhoidal and non typhoidal *Salmonella* serovars may provide important targets for vaccination therapies capable of cross-protection against non typhoidal serovars. We screened CD4⁺ T cell clones cross-reactive against non typhoidal serovars, for their ability to recognize autologous EBV-LCL pulsed with 30 different recombinant *S. Typhi* proteins conserved in *S. Typhimurium*²³ (Supplementary Table 2). We tested 184 clones from five volunteers, and identified T cell clones specific for three different proteins, namely PhoN, YiaD, PgcL (Supplementary Table 3). In particular, PhoN specific CD4⁺ T cell clones were identified in 5 out of the 7 volunteers tested, and its immunodominance was confirmed by ELISPOT analysis on frozen PBMC collected from challenged volunteers (Supplementary Fig. 7c).

To determine to what extent T cell clones cross-reactive against *S. Typhi*, *S. Paratyphi A* and *S. Typhimurium* were capable of recognizing more distantly related *Salmonellae*, 167 T cell clones were tested against autologous EBV cells infected with either a different non typhoidal serovar, *Salmonella* Enteritidis, or with a more distantly related species of *Salmonella*, *Salmonella bongori* (*S. bongori*). All but 12 of the tested T cell clones recognized *Salmonella* Enteritidis, consistent with the close phylogenetic relatedness of these two serovars (Fig. 7a-c), and 42 recognized *Salmonella bongori*, indicating that a fraction of the cross-reactive response recognizes epitopes conserved across *Salmonella* species. None of the clones specific for PhoN, YiaD and PgcL recognized cells infected with *Salmonella bongori*, consistent with the absence of these proteins in this bacterium (Fig. 7b,c).

In addition, we noticed that in volunteer T5, 11 PhoN specific T cell clones reactive against *S. Typhi* and *S. Paratyphi A* infected cells (Fig. 7d) failed to recognize cells infected with *S. Typhimurium* (Fig. 7e) or *Salmonella* Enteritidis (Fig. 7f). Epitope mapping of 22 PhoN specific clones from this volunteer, revealed that these recognized peptides spanning either of three distinct regions between aminoacid 45 to 70 (PhoN(45-70)), 95 to 120 (PhoN(95-120)) and 115 to 145 (PhoN(115-145)) (Fig. 7h,i). PhoN(45-70) and PhoN(115-145) specific clones crossreacted against the four serovars; in contrast, PhoN(95-120) specific clones failed to recognize *S. Typhimurium* and (with the exception of clone 101) *Salmonella* Enteritidis (Fig. 7g, h). The PhoN(95-120) region is polymorphic across the distinct serovars (Fig 7i), and consistent with their pathogen specificity, PhoN (95-120) specific T cell clones, recognized peptides containing both the *S. Typhi* and *S. Paratyphi A* PhoN(95-120) sequences, with lower affinity peptides containing the *S. Enteritidis* variant, and failed to respond to peptides containing the *S. Typhimurium* variant (Fig. 7j). Furthermore, confirming its unique ability to recognize cells infected with *Salmonella*

Enteritidis, clone 101 showed an increased reactivity to the *Salmonella* Enteritidis variant compared with the other PhoN(95-120) specific T cell clones.

These data, together with the identification of PhoN as an immunodominant T cell antigen broadly cross-reactive against distinct *Salmonella* serovars, provide a second example of small protein sequence variations targeted by non cross-reactive T cell responses.

Analysis of TCR CDR3 α and CDR3 β of *Salmonella* specific CD4⁺ T cell clones

Finally, we investigated whether effector responses to *Salmonella* infection were associated with the oligoclonal expansion of pathogen specific T cell receptor (TCR) clonotypes, whether these were enriched in the CD38⁺CCR7⁻ effector T cell subset, and whether specific CDR3 motifs were associated with the recognition of particular peptides.

Polyclonal analysis of the TCR β repertoire of CD38⁺CCR7⁻ cells and CD38⁻CCR7⁻ T cells in volunteers T4 and P1, showed that the CCR7⁻CD38⁺ subset was much less diverse than the CD38⁻CCR7⁻ subset (Supplementary Fig. 7a), suggestive that the former subset is populated by clonally expanded effector T cells.

We determined the HLA-II restriction and CDR3 sequence of the TCR α and TCR β chains of 33 T cell clones from participant T4 (Fig. 8a), and of 24 clones from participant P1 (Supplementary Fig. 8b). Among the analyzed T cell clones, similar to observations in a mouse model of *S. Typhimurium* infection²⁴, we found evidence of clonotype expansion, and of T cell clones harboring similar CDR3 β chains. As expected, all T cell clones sharing identical or nearly identical CDR3 β had the same specificity in term of pathogen discrimination, fine specificity (if determined) and MHC Class II restriction.

In donor T4, we identified seven expanding clonotypes. One of these clonotypes gave rise to three sequenced T cell clones selective for the *S. Typhi* CdtB(105-125:100H) peptide, and two clonotypes gave rise to four clones cross-reactive against the Typhi and Paratyphi

CdtB(105-125:H100Y). Six of the seven expanded clonotypes, and 7 additional clonotypes were also detected within the polyclonal TCR β library generated from CCR7⁺CD38⁺ T cells (Fig. 8b), and were virtually absent in the library generated from CCR7⁺CD38⁻ T cells (Fig. 8c), consistent with the segregation of pathogen specific effector cells at the peak of the immune response within the CCR7⁺CD38⁺ subset.

Expanded clonotypes were also observed in T cell clones isolated from donor P1. In this case only 6 of the 22 clonotypes characterized were identified within the CCR7⁺CD38⁺ polyclonal library, which correlates with a lower frequency of pathogen specific T cell clones identified in donor P2 compared to donor T4 (Fig. 3e,f and Supplementary Fig. 8c, d).

We extended these results to the analysis of 140 clones isolated from volunteer T5 and 79 clones isolated from volunteer T6 (Supplementary Tables 4, 5). Expanded clonotypes with as many as 7 T cell clones harboring the same TCR sequence were identified in both volunteers (Supplementary Tables 4, 5 and Fig. 8f), some of them targeting PhoN and HlyE. Furthermore, distinct specificity groups, with similar clonotypes recognizing specific HLADR-epitope combinations were also identified (Fig. 8d, e and Supplementary Table 6, 7).

The ability to match pathogen and antigen specificity with TCR sequencing data gave us the opportunity to draw snapshots of the effector response to *Salmonella* (Fig. 8f), partitioning the effector T cells based on their pathogen reactivity, protein and epitope specificity, HLA restriction and clonotype size. This analysis shows how, despite the large number of potential protein antigens, bacteria-specific T cell responses are largely associated with clonotype expansion and selection of effector T cells recognizing a limited number of specificities.

Discussion

Different studies have attempted to dissect the complexity of T cell immunity to bacteria either by high through-put screening for bacterial antigens recognized by polyclonal memory T cell responses^{25 26}, or by performing single cell sequencing to define the number of effector T cell clones activated during infection²⁴. Both approaches have important limitations: the first falls short of discriminating between recently activated and memory T cells; while the latter fails to provide information on the specificity of effector T cells. Furthermore, single cell TCR sequencing approaches do not allow to dissect and quantify cross-reactive T cell responses, which requires testing individual T cells for their capacity to respond to distinct bacterial antigens and bacterial strains.

In this study, we overcome some of the limitations of the two above approaches by focusing our analysis on effector T cells expanded as a direct result of *Salmonella* infection in human, and by defining their specificity and cross-reactivity at single cell level after *in vitro* clonal expansion.

Previous studies identified CD4⁺ T cell responses to *Salmonella* antigens in individuals with enteric fever^{27, 28}, as well as increased *ex-vivo* responses to *S. Paratyphi A* following vaccination with the *S. Typhi* attenuated strain Ty21a²⁹. However, none of these studies were capable of dissecting cross-reactive vs non cross-reactive components of the CD4⁺ T cells responses, or of identifying T cells responses targeting selectively *S. Typhi* or *S. Paratyphi A* specific antigens compared with antigens shared by multiple *Salmonella* serovars.

In this study, we have identified frequent antigen specific T cell responses to three distinct *Salmonella* antigens: HlyE, CdtB and PhoN. HlyE is a hemolysin, whose role in the pathogenicity of *Salmonella* is currently unclear³⁰.

CdtB is the catalytic component of the Typhoid toxin, which has been proposed as a key virulence factor in the pathogenicity of *S. Typhi* and Paratyphi A¹⁸ and is considered a major target for vaccination strategies against enteric fever aimed at blocking the symptoms caused by the bacteria³¹. Our finding suggest that CdtB could be put forward as a candidate vaccine to elicit both antibody responses capable of neutralizing the toxin activity, as well as T cell responses targeting infected cells. However, since CdtB fail to elicit fully cross-reactive responses against the two serovars, both *S. Typhi* and Paratyphi A CdtB proteins should be used to generate optimal CD4⁺ T cell responses targeting both serovars.

PhoN is an acid phosphatase induced upon activation of the two-component regulatory system PhoP-PhoQ³², one of the molecular rheostats controlling the transcriptional switch associated with invasion of target cells.

The broad cross-reactivity of PhoN specific T cell responses against both pathogenic typhoidal and non-typhoidal serovars makes this antigen of interest not only for the development of broadly cross-reactive candidate vaccines, but also as a tool to measure broadly cross-reactive immunity to *Salmonella* upon infection and vaccination.

Importantly, *Salmonella* CD4⁺ T cell response targets proteins constitutively expressed by the bacterium, but also proteins induced only upon infection, demonstrating how the antigen specific repertoire of CD4⁺ T cells is shaped by the transcriptional plasticity of *Salmonella*, and how antigen expressed only in the infected tissue are a major target of the CD4⁺ T cell response to *Salmonella*.

S. Typhi and Paratyphi A invade systemically through the gut mucosa. Many of the CD4⁺CD38⁺CCR7⁻ T cells expressed the gut homing markers CD49d and Integrin-β7, suggesting that circulating effector T cells might have the capacity to migrate to the site of bacteria colonization, and join the pool of tissue resident CD4⁺ T cell which patrol the gut mucosa. Gut resident CD4⁺ T cells are likely to play an important role in protection against

reinfection, and future studies will be needed to investigate whether infection or vaccination shape the antigen specific repertoire as well as the frequency of *Salmonella* specific tissue resident CD4⁺ T cells.

In conclusion, in this study we have described a novel approach to interrogate the specificity and clonality of bacterial specific T cells, and demonstrated with unprecedented details that the antigen specific repertoire of CD4⁺ T cells activated during *Salmonella* infection includes both largely cross-reactive and serovar specific T cell clonotypes. and is shaped by small aminoacid variations in immunodominant T cell antigens (such as CdtB and PhoN). Our findings highlight the importance of dissecting the target discrimination potential of effector T cell clones to identify cross-reactive and non cross-reactive responses to infection. By characterizing novel immunodominant T cells antigens, these findings pave the way for the design of vaccination strategies capable of eliciting serovar specific and cross-reactive T cell responses. In addition, the development of new tools to identify typhoidal specific immune responses provides new diagnostic targets to assess T cell immunity induced upon natural immunity or vaccination against distinct *Salmonella* serovars.

Acknowledgments

This work was supported by the UK Medical Research Council (MRC) (MR/K021222/1), Cancer Research UK (CRUK) (C399/A2291), the NIHR Clinical Research Network Thames Valley, Oxford Biomedical Research Centre, Bill & Melinda Gates Foundation (OPP1084259), the European Vaccine Initiative (PIM) and core funding from the Singapore Immunology Network (SIgN) and the SIgN immunomonitoring platform. GD is supported by The Wellcome Trust. We thank C. Waugh and WIMM FACS facility for assistance with cell sorting, T. Rostron for assistance with next generation sequencing. The DRB4 Tetramers were provided by B. Kwok and I-T. Chow, from the Tetramer Core Laboratory at the Benaroya Research Institute at Virginia Mason.

Authors contribution

G.N. conceived and designed the study, processed the samples, performed and supervised the experiments, analyzed the data and wrote the manuscript. P.K., processed the samples, performed experiments, and analyzed the data. L.H., P.d.H, L.P.-L., L.S., M.S., assisted with experiments. A.A. designed and performed bacteria-macrophage co-culture experiments. M.R. and D.M.S.P. optimized and performed TCR repertoire experiments and analysis. K.W.W.T, E.B., M.T.W. E.W.N developed the metal conjugated antibody panels, coordinated and performed the Mass Cytometry experiments, and provided assistance with the analysis of Mass Cytometry experiments. A.J.P conceived the human challenge model development, and directed the clinical trial. H.D., M.M.G., designed and directed the clinical trial. D.C., C.J., C.J.B. coordinated the clinical trial and sampling. C.J., H.T.-B., H.B.J., coordinated sampling and processed samples. L.R.O. designed peptide pools of overlapping peptides. S.B., G.D., D.B., D.P. provided reagents. G.N., M.A.G., A.S., V.C., A.J.P., coordinated the study. V.C. conceived and designed the study, edited the manuscript and

supervised the experiments. All authors discussed the results and commented on the manuscript.

Data availability.

The data that support the findings of this manuscript are available from the corresponding authors upon request.

Mass Cytometry fcs files from this paper are available in the Flow Repository:

<http://flowrepository.org/id/FR-FCM-ZYW2>

Raw data of the analysis of the TCR repertoire of CD38+CCR7- cells are available at the Gene Expression Omnibus (GEO). Accession Number GSE113112

<https://www.ncbi.nlm.nih.gov/geo/query/acc.cgi?acc=GSE113112>

Competing Interests

The authors declare no competing interests.

References

1. Crump, J.A., Luby, S.P. & Mintz, E.D. The global burden of typhoid fever. *Bull World Health Organ* **82**, 346-353 (2004).
2. Crump, J.A. & Mintz, E.D. Global trends in typhoid and paratyphoid Fever. *Clin Infect Dis* **50**, 241-246 (2010).
3. Mogasale, V. *et al.* Burden of typhoid fever in low-income and middle-income countries: a systematic, literature-based update with risk-factor adjustment. *Lancet Glob Health* **2**, e570-580 (2014).
4. Dougan, G. & Baker, S. Salmonella enterica serovar Typhi and the pathogenesis of typhoid fever. *Annu Rev Microbiol* **68**, 317-336 (2014).
5. Gal-Mor, O., Boyle, E.C. & Grassl, G.A. Same species, different diseases: how and why typhoidal and non-typhoidal Salmonella enterica serovars differ. *Front Microbiol* **5**, 391 (2014).
6. McClelland, M. *et al.* Comparison of genome degradation in Paratyphi A and Typhi, human-restricted serovars of Salmonella enterica that cause typhoid. *Nat Genet* **36**, 1268-1274 (2004).
7. Holt, K.E. *et al.* Pseudogene accumulation in the evolutionary histories of Salmonella enterica serovars Paratyphi A and Typhi. *BMC Genomics* **10**, 36 (2009).

8. Coward, C. *et al.* The effects of vaccination and immunity on bacterial infection dynamics in vivo. *PLoS Pathog* **10**, e1004359 (2014).
9. Griffin, A.J. & McSorley, S.J. Development of protective immunity to Salmonella, a mucosal pathogen with a systemic agenda. *Mucosal Immunol* **4**, 371-382 (2011).
10. Lee, S.J., Dunmire, S. & McSorley, S.J. MHC class-I-restricted CD8 T cells play a protective role during primary Salmonella infection. *Immunol Lett* **148**, 138-143 (2012).
11. Dunstan, S.J. *et al.* Variation at HLA-DRB1 is associated with resistance to enteric fever. *Nat Genet* **46**, 1333-1336 (2014).
12. Waddington, C.S. *et al.* An outpatient, ambulant-design, controlled human infection model using escalating doses of Salmonella Typhi challenge delivered in sodium bicarbonate solution. *Clin Infect Dis* **58**, 1230-1240 (2014).
13. McCullagh, D. *et al.* Understanding paratyphoid infection: study protocol for the development of a human model of Salmonella enterica serovar Paratyphi A challenge in healthy adult volunteers. *BMJ Open* **5**, e007481 (2015).
14. Blohmke, C.J. *et al.* Interferon-driven alterations of the host's amino acid metabolism in the pathogenesis of typhoid fever. *J Exp Med* **213**, 1061-1077 (2016).
15. Levine, J.H. *et al.* Data-Driven Phenotypic Dissection of AML Reveals Progenitor-like Cells that Correlate with Prognosis. *Cell* **162**, 184-197 (2015).
16. Krutzik, P.O. & Nolan, G.P. Fluorescent cell barcoding in flow cytometry allows high-throughput drug screening and signaling profiling. *Nat Methods* **3**, 361-368 (2006).
17. Haghjoo, E. & Galan, J.E. Salmonella typhi encodes a functional cytolethal distending toxin that is delivered into host cells by a bacterial-internalization pathway. *Proc Natl Acad Sci U S A* **101**, 4614-4619 (2004).
18. Song, J., Gao, X. & Galan, J.E. Structure and function of the Salmonella Typhi chimaeric A(2)B(5) typhoid toxin. *Nature* **499**, 350-354 (2013).
19. Liang, L. *et al.* Immune profiling with a Salmonella Typhi antigen microarray identifies new diagnostic biomarkers of human typhoid. *Sci Rep* **3**, 1043 (2013).
20. Rodriguez-Rivera, L.D., Bowen, B.M., den Bakker, H.C., Duhamel, G.E. & Wiedmann, M. Characterization of the cytolethal distending toxin (typhoid toxin) in non-typhoidal Salmonella serovars. *Gut Pathog* **7**, 19 (2015).
21. von Rhein, C. *et al.* ClyA cytolysin from Salmonella: distribution within the genus, regulation of expression by SlyA, and pore-forming characteristics. *Int J Med Microbiol* **299**, 21-35 (2009).

22. Oscarsson, J. *et al.* Characterization of a pore-forming cytotoxin expressed by *Salmonella enterica* serovars typhi and paratyphi A. *Infect Immun* **70**, 5759-5769 (2002).
23. Barat, S. *et al.* Immunity to intracellular *Salmonella* depends on surface-associated antigens. *PLoS Pathog* **8**, e1002966 (2012).
24. Stubbington, M.J. *et al.* T cell fate and clonality inference from single-cell transcriptomes. *Nat Methods* **13**, 329-332 (2016).
25. Lindestam Arlehamn, C.S. *et al.* Memory T cells in latent *Mycobacterium tuberculosis* infection are directed against three antigenic islands and largely contained in a CXCR3+CCR6+ Th1 subset. *PLoS Pathog* **9**, e1003130 (2013).
26. Bhuiyan, S. *et al.* Cellular and cytokine responses to *Salmonella enterica* serotype Typhi proteins in patients with typhoid fever in Bangladesh. *Am J Trop Med Hyg* **90**, 1024-1030 (2014).
27. Reynolds, C.J. *et al.* The serodominant secreted effector protein of *Salmonella*, SseB, is a strong CD4 antigen containing an immunodominant epitope presented by diverse HLA class II alleles. *Immunology* **143**, 438-446 (2014).
28. Sheikh, A. *et al.* Interferon-gamma and proliferation responses to *Salmonella enterica* Serotype Typhi proteins in patients with S. Typhi Bacteremia in Dhaka, Bangladesh. *PLoS Negl Trop Dis* **5**, e1193 (2011).
29. Wahid, R., Fresnay, S., Levine, M.M. & Sztein, M.B. Cross-reactive multifunctional CD4+ T cell responses against *Salmonella enterica* serovars Typhi, Paratyphi A and Paratyphi B in humans following immunization with live oral typhoid vaccine Ty21a. *Clin Immunol* **173**, 87-95 (2016).
30. Fuentes, J.A., Villagra, N., Castillo-Ruiz, M. & Mora, G.C. The *Salmonella* Typhi hlyE gene plays a role in invasion of cultured epithelial cells and its functional transfer to S. Typhimurium promotes deep organ infection in mice. *Res Microbiol* **159**, 279-287 (2008).
31. Galan, J.E. Typhoid toxin provides a window into typhoid fever and the biology of *Salmonella* Typhi. *Proc Natl Acad Sci U S A* **113**, 6338-6344 (2016).
32. Groisman, E.A. The pleiotropic two-component regulatory system PhoP-PhoQ. *J Bacteriol* **183**, 1835-1842 (2001).

Figure legends

Figure 1. Mass cytometry identification of effector CD4⁺ T cells responding to *Salmonella* infection: (a) Human Challenge Model of typhoidal *Salmonella* infection and sample collection time points. Enteric fever (EF) time point corresponds to 2-4 days after clinical diagnosis of enteric fever. In the analyzed volunteers diagnosis was between day 6 and day 12 (Median= 8 days); (b) Frequency of Ki67⁺ cells over time within CD4⁺ T cells in frozen PBMC analyzed by Mass Cytometry (n=6). Friedman Test p=0.0342, Dunn's Multiple Comparison Test day 0 (D0) vs day 4 (D4), day 28 (D28), day 90 (D90) =ns, D0 vs EF =0.02247; (c) t-distributed stochastic neighbor embedding (tSNE) map describing the heterogeneity of Ki67⁺CD4⁺ T cells identified in all volunteers (n=6, 5 time points). Cells are colored by cell-type assignments detected by PhenoGraph; (d) Heatmap showing the hierarchical clustering of samples based on the frequency of the distinct PhenoGraph Ki67⁺ subsets at different time points. Each column represents one of the 30 samples analyzed. (e) Heatmap describing the relative expression of each marker within cluster 19, compared with its expression in the other clusters. Median expressions of the distinct phenotypic markers were normalized, scaled across clusters and then ranked from top to bottom based on their z-score value in cluster 19; (f) Counter plot describing the frequency of CD38⁺CCR7⁻CD4⁺ T cells detected by Mass Cytometry at D0 and EF in one representative volunteer, and (g) cumulative frequency of this population across different time points (n=6). Friedman Test p=0.0019, Dunn's Multiple Comparison Test D0 vs D4, D28, D90 =ns, D0 vs EF =0.0021. (b,g) Box extends from the 25th to the 75th percentile and whiskers from the minimum to the maximum value; line indicates median.

Figure 2. CD38⁺CCR7⁻CD4⁺ T cells contain a homogenous population of IFN γ ⁺ MIP-1 β ⁺ producing cells: (a) Bivariate plots showing expression of different cytokines and activation markers in CD38⁺CCR7⁻CD4⁺ T cells compared to memory CD45RA⁻CD38⁻CD4⁺ T cells in PBMC stimulated for 4h with PMA/Ionomycin in the presence of Brefeldin A and Monensin (one representative volunteer out of four).

(b) Frequency of T cells expressing the indicated cytokines and activation markers within CD4⁺CD45RA⁻ and CD4⁺CD38⁺CCR7⁻ T cells (n=4). Two-tailed paired t-test was applied to compare frequency of cells expressing the indicated cytokines/markers within the two distinct subsets: IFN- γ p=0.0119, CD40L p=0.0156, CTLA4 p=0.0081, IFN- γ p=0.0119, Mip-1 β p=0.0062, TNF p=0.083; * p<0.05, ** p<0.01. (c) tSNE plots generated based on the analysis of cytokines and activation markers, and color-coded according to the relative

expression of the indicated markers. **(d)** Overlay of the memory and effector (CD38⁺CCR7⁻) T cell populations in one representative individual and gating of multifunctional (MF) effector cells **(e)** Frequency of MF effector cells within CD38⁺CCR7⁻ T cells and total CD45RA⁺ T cells in four volunteers (n=4) during enteric fever. Two-tailed paired t-test: * p=0.028. **(b,e)** Box extends from the 25th to the 75th percentile and whiskers from the minimum to the maximum value; line indicates median.

Figure 3. Analysis of libraries of CD38⁺CCR7⁻ T cell clones and fluorescent barcoding to dissect the antigen specific repertoire of effector CD4⁺ T cells.

(a) Effector CD4⁺ T cells were FACS sorted as individual T cell, expanded with PHA and IL-2 in the presence of irradiated feeders and then tested for their capacity to recognize *Salmonella* infected autologous lymphoblastoid cell lines.

(b) Schematic example of fluorescent cell barcoding to test and compare the specificity of different T cell clones. Clones were labelled with distinct dilutions of 3 different fluorescent dyes, pooled and co-cultured for 6h with autologous EBV transformed B cell lines pulsed with a recombinant antigen, or infected with a *Salmonella* serovar. Brefeldin A was added for the last 4 hours of stimulation. Shown is the different response measured as intracellular cytokine staining of IFN- γ by two clones in the presence of two distinct stimulatory conditions.

(c) T cell clones were generated from CD38⁺CCR7⁻ or CD38⁻CCR7⁻ CD4⁺ T cells isolated 2 days after diagnosis from *S. Typhi* infected volunteers T1 and T2.

Shown are the proportion of *S. Typhi* specific T cell clones within the total of the expanding clones and **(d)** the IFN- γ response (depicted as % of IFN- γ positive cells in intracellular cytokine staining) of the different clones in the presence of autologous EBV-LCL infected with *S. Typhi* (Quailes strain) (T1: CD38⁺CCR7⁻ n=51, CD38⁻CCR7⁻ n=22) (T2: CD38⁺CCR7⁻ n=51, CD38⁻CCR7⁻ n=29). One-tailed Mann-Whitney test, **** p<0.0001, * p=0.0107 **(e)** Pie charts show the proportion of CD38⁺CCR7⁻CD4⁺ T cell clones recognizing EBV-LCL infected with *S. Typhi* (Ty21a strain) in six *S. Typhi* infected volunteers, and **(f)** EBV-LCL infected with *S. Paratyphi* A (NVGH308) in two *S. Paratyphi* A infected volunteers.

Figure 4. Cross-reactivity of *Salmonella* specific CD4⁺ T cell clones against different *Salmonella* Serovars.

(a) IFN- γ production by three representative clones (out of a total of 507 *Salmonella* specific clones analysed) isolated from a *S. Typhi* infected volunteer in the presence of only autologous EBV-LCL, or EBV-LCL infected with *S. Typhi* (Quailes), *S. Paratyphi* A (NVGH308) or *S. Typhimurium* (LT2). (b-d) Plots describing the cumulative response of 87 CD38⁺CCR7⁻ CD4⁺ T cell clones isolated from *S. Typhi* challenged volunteer T4, in the presence of EBV-LCL infected with different *Salmonella* serovars. Each dot represents IFN- γ production measured by intracellular cytokine staining by an individual T cell clone in response to EBV-LCL infected with: (b) two distinct strains of *S. Typhi* (the challenge strain Quailes and the recombinant attenuated strain BRD948); (c) the *S. Typhi* challenge strain Quailes and the *S. Paratyphi* A challenge strain NVGH308, (d) the Quailes strain of *S. Typhi* and the *S. Typhimurium* strain LT2. Data are representative of 8 volunteers analysed. (e) Venn diagram describing the number of T cell clones isolated from the different *Salmonella* infected volunteers, recognizing cells infected with one or more of the different Serovars.

Figure 5. HlyE and CdtB are *S. Typhi* and *S. Paratyphi* A specific immuno-dominant T cell antigens.

(a) IFN- γ production by *S. Typhi* specific T cell clones (n=44) non cross-reactive against *S. Typhimurium* from volunteer T4 stimulated with HlyE and CdtB peptide pools. Red and blue dots represent HlyE and CdtB specific clones, respectively. (b) IFN- γ production by CdtB (blue dots) and HlyE (red dots) specific T cell clones in response to EBV-LCL infected with *S. Typhi* (Quailes strain) or *S. Typhimurium* (LT2 strain) among the total of CD4⁺ CD38⁺CCR7⁻ clones isolated from volunteer T4 (n=87). (c) Proportion of HlyE and CdtB specific T cell clones among T cell clones non cross-reactive against *S. Typhimurium*, but specific for typhoidal serovars across 8 different volunteers. (d) IFN- γ production by T cell clones (n=87) generated from volunteer T4 in response to *S. Typhi* strains Quailes and Ty21a, red dots represent HlyE specific clones. (e) IFN- γ production by T cell clones generated from volunteer T4 in response to recombinant HlyE, and autologous EBV-LCL infected with *S. Paratyphi* A (NVGH308 strain), *S. Typhi* Quailes strain (*S. Ty*), *S. Typhi* Ty21a strain (Ty21a), and *S. Typhimurium* LT2 strain. Red dots represent HlyE specific T cell clones. One-way ANOVA, p=0.0021, Tukey's multiple comparison test: NVGH308 vs

Ty21a $p=0.0216$, Quailes vs Ty21a $p=0.0005$, Quailes vs NVGH308 $p=0.036$. Box extends from the 25th to the 75th percentile and whiskers from the minimum to the maximum value; line indicates median.

(f) Kinetic of mRNA expression (plotted as Arbitrary Unit compared to 16S rRNA) of CdtB in *S. Typhi* infected EBV-LCL. Data representative of two independent experiments. (g) IFN- γ production by T cell clones ($n=87$) isolated from volunteer T4 in the presence of autologous EBV LCL infected with live *S. Typhi* (BRD948 strain) or pulsed with a lysate of *S. Typhi* (BRD948 strain). Red dots represent CdtB specific T cell clones. Data representative of clones from two volunteers. Data representative of two independent experiments, in two volunteers.

Figure 6. Sequence dependent recognition of different *Salmonella* serovars by CdtB specific T cell clones.

(a) IFN- γ production of CdtB specific T cell clones from volunteer T4 in the presence of autologous EBV-LCL infected with *S. Typhi* and *S. Paratyphi A*. Red dots represent CdtB specific clones recognizing only *S. Typhi* infected cells and blue dots represent CdtB specific clones recognizing EBV-LCL infected with both *S. Typhi* or *S. Paratyphi A*. (b) Aminoacid sequence of CdtB in *S. Typhi* (Quailes) and *S. Paratyphi A* (NVGH308). (c) IFN- γ production by CdtB specific cross-reactive (blue dots, $n=5$) and non cross-reactive (red dots, $n=6$) from volunteer T4 in the presence of the CdtB(105-125) peptide containing either the *S. Typhi* or the *S. Paratyphi A* sequence. Mann Whitney two tailed t-test **: $p=0.0043$. Shown are median and interquartile range. (d) IFN- γ production from T cell clones from volunteer P1 in response to EBV-LCL infected with *S. Typhi*, *S. Paratyphi A*, or stimulated with CdtB peptide pool. Clone 99 is depicted in red, Clone 106 depicted in blue. (e) IFN- γ production by Clone 99 (red) and Clone 106 (blue) from volunteer P1 in the presence of different CdtB peptides. (d,e) Data are representative of two independent experiments. (f) Staining of a *S. Typhi* specific (red), *S. Paratyphi* specific (green) and cross-reactive (blue) CdtB(105-125) specific T cell clones with HLADRB4 tetramers loaded with either the CdtB(105-125)SP110H (DRB4*SP110H) or the CdtB(105-125)ST110Y (DRB4*ST110Y) peptide variants. Stainings are representative of 8 CdtB specific clones tested. (g) *Ex-vivo* frequency of combined HLADRB4 tetramer positive T cells

(PE⁺∪APC⁺∪PE⁺APC⁺ cells) 28 days after challenge compared to baseline in volunteers (n=12) challenged with *S. Typhi* (black dots) and *S. Paratyphi A* (red dots). Wilcoxon matched pairs signed rank test. *** p=0.0005. (h) *Ex-vivo* HLADRB4 tetramer staining of frozen PBMC collected 28 days after challenge with *S. Typhi* or *S. Paratyphi* from two representative volunteers identifying CD4⁺ T cells decorated by the DRB4*SP110H tetramer (lower right quadrant) or the DRB4*ST110Y (upper left quadrant) or both (upper right quadrant). Number within each quadrant represent the % of CD4⁺ T cells labeled by the distinct tetramers. (i) Proportion of CD4⁺ tetramer positive cells stained *ex-vivo* with DRB4*SP110H, DRB4*ST110Y or both DRB4 tetramers in frozen PBMC collected from different volunteers 28 days after challenge with *S. Typhi* or *S. Paratyphi A*. Color coding as indicated in panel f. Mann-Whitney Two Tailed Test for the difference in the proportion of ST110H⁺ cells in *S. Typhi* (n=6) compared to *S. Paratyphi A* (n=6) challenged volunteers p=0.0022, and in the proportion of SP110Y⁺ in *S. Paratyphi A* compared to *S. Typhi* p=0.005.

Figure 7. Characterization of the specificity of T cell clones cross-reactive against non typhoidal *Salmonella*.

(a,b) Cross-reactivity of *S. Typhimurium* specific CD4⁺ T cell clones (n=167) against *S. Enteritidis* and *S. bongori*. PhoN specific T cell clones are depicted as red dots, YiaD specific T cell clones as green dots, and PgcL specific T cell clones as blue dots. (c) Venn diagram depicting the number of cross-reactive T cell clones recognizing *S. Typhimurium* infected cells that can also recognize *S. Enteritidis* (113 clones), and both *S. Enteritidis* and *S. bongori* (43 clones). (d-e-f) IFN- γ production from PhoN specific T cell clones from volunteer T5 in the presence of cells infected with *S. Typhi* vs *S. Paratyphi A* (d), *S. Typhi* vs *S. Typhimurium* (e), and *S. Typhi* vs *S. Enteritidis* (f). (g-h) IFN- γ production from 22 T cell clones specific for distinct PhoN epitopes (aa 45-70, 95-120, 115-145) in the presence of cells infected with *S. Typhi* vs *S. Typhimurium* (g) and *S. Typhi* vs *S. Enteritidis* (h) Arrows indicates clone 101. (i) Sequence of PhoN(95-120) in *S. Typhi*, *S. Paratyphi A*, *S. Typhimurium* and *S. Enteritidis*. (j) IFN- γ production by PhoN (95-120) specific T cell clones (n=7) in the presence of the 95-115 and 100-120 *S. Typhi* (Ty), *S. Paratyphi* (P), *S. Enteritidis* (E) and *S. Typhimurium* (Tym) peptide variants. Red dots represent *S. Enteritidis* reactive clone 101. Friedman multiple comparison test (p<0.0005), and Dunn's multiple

comparison test of IFN- γ production in the presence of peptide containing the *S. Typhi* variant compared to the *S. Paratyphi A*, *S. Typhimurium* or *S. Enteritidis* variants.

Figure 8. Clonal expansion of Salmonella specific effector T cells.

(a) Pathogen selectivity, antigen specificity, HLA restriction, TCR CDR3 α and CDR3 β sequence of T cell clones isolated from volunteer T4. Colored sequences were identified also in the TCR β repertoire of CD38⁺CCR7⁻ T cells from the same volunteer. (b) Pie Chart depicting the frequency (as fraction of total sequences identified) of CDR3 β sequences within the TCR β repertoire of CD38⁺CCR7⁻ T cells (9130 cells probed) from volunteer T4. Highlighted are the CDR3 β sequences identified also in the isolated T cell clones. (c) Frequency of CDR3 β sequences within the polyclonal repertoire of CD38⁺CCR7⁻ T cells and CCR7⁻CD38⁻ (1.3×10^5 cells probed) T cells in volunteer T4. Red circles indicated CDR3 β sequences of clones highlighted in panel b. (d) Similar CDR3 α and CDR3 β motifs in HlyE specific T cell clones in donor T6. 4 of the 5 clonotypes were characterized as HlyE(40-65) specific, the fine specificity of the fifth was not determined (HlyE?). Indicated is also the number (N) of clones with the same TCR sequence identified in our screening. (e) Similar CDR3 β sequences in HLA DRB1*0701 restricted HlyE(155-175) specific T cell clones from volunteer T6 and P1. (f) Diagram describing the pathogen specific T cell repertoire of the representative volunteer T6. Circles represent distinct clonotypes, with size proportional to the number of clones with that specific clonotype identified, and colors indicating the HLA-class II restriction (when determined). Clonotypes are grouped based on pathogen selectivity (continuous line) and protein specificity (dashed line).

Material and Methods

Human challenge model

Samples were collected from healthy community adult volunteers in two controlled human infection studies conducted at the Centre for Clinical Vaccinology and Tropical Medicine, Oxford, United Kingdom (ClinicalTrials.gov identifiers NCT02100397 and NCT02192008). Details of study protocols and enrolment criteria were as described elsewhere ^{12, 33} Briefly, participants underwent oral challenge with *S. Typhi* Quail's strain (10^4 CFU) or *S. Paratyphi* A NVGH308 (10^3 CFU) suspended in a NaHCO₃ solution (0.53g/30ml) following neutralization of stomach acid.

Participants were monitored in an outpatient setting with daily clinical review and collection of blood and stool cultures. A diagnosis of enteric fever was defined as *S. Typhi* or *S. Paratyphi* bacteremia identified between Day 3 to Day 14 post-challenge and/or a persistent fever $\geq 38^\circ\text{C}$ for ≥ 12 hours. Individuals not meeting the pre-specified diagnostic criteria were commenced on antibiotics at Day 14 and were defined as not-diagnosed. The studies were approved by Oxfordshire Research Ethics Committee A (14/SC/0004 and 14/SC/1204) and performed according to the provisions of the Declaration of Helsinki and Good Clinical Practice guidelines.

Stimulation, Staining, and CyTOF Data Acquisition

CyTOF analysis was performed in order to identify cellular signatures in the CD4⁺ T cell response associated with enteric fever. For this reason, samples were selected based on sample availability and high bacterial load at diagnosis. No sample selection was performed for subsequent analysis (whole blood staining, ELISPOT, Tetramer staining, and clone isolation). Cryopreserved samples were thawed and washed with pre-warmed RPMI supplemented with 10% FBS (GIBCO, Life Technologies), 1X Penicillin/Streptomycin/L-glutamine (GIBCO, Life Technologies), 1% 1M HEPES (GIBCO, Life Technologies) and 1X β -mercaptoethanol (GIBCO, Life Technologies). Cells from each sample were split into two wells, followed by staining with the indicated antibodies (Supplementary Table 1) in 96-well round bottom plates for 30 minutes at 37°C prior to stimulation. Cells were left untreated or stimulated at 37°C for 4 hours with 150 ng/ml phorbol-12-myristate-13-acetate (PMA) (Sigma-Aldrich) and 1 μM ionomycin (Sigma-Aldrich) in the presence of monensin and Brefeldin A (eBioscience).

After stimulation, cells were washed twice in cold PBS, followed by incubation on ice with 200 μ M cisplatin (Sigma-Aldrich) for 5 minutes. Cells were then washed with CyFACS buffer (PBS + 4% FBS + 0.05% sodium azide) and stained with streptavidin- α Galcer with 10 μ M free biotin for 30 minutes at room temperature. This was followed by 30 minutes incubation in primary antibody cocktail on ice. Cells were then washed twice in CyFACS and stained with metal-tagged surface antibodies. After 30 minutes, stimulated cells were washed twice with CyFACS, once with PBS, and then fixed in 2% paraformaldehyde (PFA; Electron Microscopy Sciences) at 4°C. The untreated cells were washed twice with CyFACS and incubated in Foxp3 Fixation/Permeabilization buffer (eBioscience) on ice for 30 minutes. Cells were then washed twice in 1 x Permeabilization (perm) Buffer (Biolegend) and stained with biotin anti-human Foxp3 and metal-tagged intracellular antibodies for 30 minutes on ice. After washing twice with perm buffer, cells were incubated on ice with metal-tagged streptavidin for 10 minutes. Cells were then washed twice in perm buffer, once in PBS, and then fixed in 2% PFA at 4°C. The next day, stimulated cells were washed twice with perm buffer and stained with intracellular antibodies on ice. After 30 minutes, all the untreated and stimulated cells were washed twice with perm buffer and once with PBS. Cells were then incubated with cellular barcodes for 30 minutes as previously described ³⁴.

Pt-102, Rh-103, Pd-104, -105, -106, -108 and -110 were used for this experiment. 113 was not used due to interference with CD57 on mass 115, based on our observations from previous experiments. A small degree of interference was observed between 110 and 112/114 but this did not affect de-barcoding as we could easily gate on 110 positive cells without including 112/114 positive cells. In addition, since CD14 positive cells (112 and 114 positive) were excluded for analysis, interference between 110 and 112/114 was not an issue. Cells were then washed once with perm buffer and incubated in CyFACS for 10 minutes on ice. Cellular DNA was labeled at room temperature with 250 nM iridium interchelator (Fluidigm) diluted in PBS with 2% PFA. After cellular DNA labeling cells were washed twice with CyFACS and kept in a 96 well U-bottom plate.

To accommodate the required numbers of samples, two barcoded batches were prepared, ensuring each batch included all time-points for a given volunteer. A single healthy donor's PBMCs, that was prepared and stained in parallel with volunteer samples, was included in each batch as a control for batch-to-batch variation.

For acquisition, small aliquots of cells from each batch were filtered through a 0.35 μm cell strainer into a 5 mL polystyrene tube. The batch aliquot was then washed twice in water before being resuspended in water at 500,000 cells/mL. EQ Four Element Calibration Beads (Fluidigm) were added at a final concentration of 1% prior to sample acquisition. The same pooling steps were repeated each time the acquisition of an aliquoted batch was completed. This approach was taken to minimize the duration the stained cells were kept in water (1–2 hours maximum).

Both batches of samples were acquired on subsequent days to minimize batch effects which can occur if stained cells are stored in CyFACS long term. Batch effect was analyzed by performing a tSNE plot to compare the PBMCs from the healthy donor stained and acquired with the two distinct batches. Cells acquisition was performed on a CyTOF2 (Fluidigm) and the total number of live cells acquired for each sample was between 30,000–100,000.

Data Analysis:

After mass cytometry acquisition, data were exported in flow-cytometry file (FCS) format, normalized³⁵ and events with parameters having zero values were randomized using a uniform distribution of values between minus-one and zero. Each sample containing a unique combination of two metal barcodes was de-convoluted using manual gating in FlowJo to select cells stained with two and only two barcoding channels.

Heterogeneity of CD4⁺Ki67⁺ cells was evaluated with the Phenograph algorithm¹⁵ embedded in the Bioconductor CyTOFkit package³⁶. A total of 1143546 CD4 T cells was analysed (Min=4037, Max=74061, Median=31045) from which a total of 6185 Ki67⁺ cells (Min=15, Max=470, Median=148.5; for samples at the peak of Ki67⁺ cells accumulation: Min=234, Max=470) was extracted using FlowJo and analysed by Phenograph.

tSNE analysis of CD4⁺ T cells stimulated with PMA/Ionomycin was performed using Cytobank³⁷ on a total of 224091 (Min=2005, Max= 35706, Median=9840) CD4⁺CD45RA⁺ T cells from volunteers 6, 22 49 and 72, at time points D0, ED and D28, based on the expression of CD40L, CTLA-4, MIP-1 β , TNF, IFN- γ , IL-2, GM-CSF, IL-17, IL-22, CD107a, IL-4, IL-8 and IL-10. At the peak of the response 347 (Donor 22), 219 (Donor 49), 346 (Donor 6) and 398 (Donor 72) CCR7⁻CD38⁺ events were identified.

Medium, reagents and strains

The medium used throughout was RPMI 1640 (Gibco) supplemented with 2 mM L-glutamine, 1% non-essential amino acids, 1% sodium pyruvate, 1% pen/strep, 5×10^{-5} 2ME (all from Gibco) and serum: 10% FCS (Sigma) or 5% Human AB Serum (Sigma) for T cell clones.. T cell clones medium was supplemented with 1000U/ml recombinant human IL-2, produced in our laboratory as described ³⁸.

Purified Phytohemagglutinin (PHA) (Remel), Ionomycin (Sigma), Phorbol 12-myristate 13-acetate PMA (Sigma), Cyclosporin B (Sigma), Gentamycin (ThermoFisher Scientific), Brefeldin A (Biolegend).

Autologous Epstein Barr virus (EBV)-transformed lymphoblastoid cell lines (EBV-LCL) were generated from PBMC collected before challenge, by incubation with supernatant from B95-8 Marmoset cells in the presence of 2 μ g/ml of Cyclosporin A (Sigma).

Bacterial strains were *S. Typhimurium* LT2 and D23580, *S. Typhi* BRD948 (Ty2 Δ aroC aroD htrA), Quailes and Ty21a, *S. Paratyphi* A NVGH308, *Salmonella bongori* (M07), *Salmonella* Enteritidis.

T cell cloning and live fluorescent barcoding

Individual cells were sorted in 96 well round bottom plate containing 125000 feeders cell/well in 150 μ l of RPMI medium containing Pen/Strep, Glutamine, NNAA, Sodium Piruvate, beta mercaptoethanol, 1000u/ml of IL-2 supernatant and Human Serum (Blood bank). Clones were expanded for 4-5 weeks and then tested for their specificity as follows.

Clones were collected and incubated overnight in the absence of IL-2. The next morning clones were washed 3 times in PBS, and labelled for 10 minutes in the presence of distinct dilution and combination of CellTrace™ CFSE Cell Proliferation Kit, CellTrace™ Far Red Cell Proliferation Kit, CellTrace™ Violet Cell Proliferation Kit, CellTracker™ Orange CMTMR Dye (all from ThermoFisher Scientific). Labelling was quenched with an equal volume of Fetal Calf Serum (Gibco), clones were washed 5 times in RPMI 10% FCS, and left to rest at 37C for 1-2h. After resting clones were pooled, counted and then incubated at 10^6 cells/ml in the presence of 1 μ g/ml Brefeldin A with either 3×10^5 /ml autologous EBV cells lines infected overnight with *Salmonella* or pulsed overnight with 10ug/ml recombinant proteins, or incubated with 5ug/ml peptide pool of CdtB and HlyE.

After 6h stimulation cells were fixed, permeabilized and stained with anti CD4 (RPA-T4) PerCP-Cy5.5 (Biolegend), CD3 PE-Cy7 (Biolegend), and IFN- γ APC-e780 (eBioscience).

Samples were then acquired using a BD FACS CANTO II flow cytometer, or a X50 BD Symphony machine and analysed with Flowjo 10 (TreeStar). Viability was assessed with live/dead Aqua staining, according to the manufacturer's instructions (Life Technologies). T cell clones were considered positive with IFN- γ^+ > 5% in the presence of bacteria infected autologous cells, and/or IFN- γ^+ > 20% in the presence of cells pulsed with proteins or peptide pools. For two of the volunteers (T4 and P2) the threshold of IFN- γ production in the presence of bacteria infected with autologous cells was increase to 10% because of higher background IFN- γ production. While some T cell clones expanded extensively and were capable to withstand several restimulation cycles, other expanded only to provide enough cell for the intial preliminary screenings of antigen specificity (which included in all cases HlyE, CdtB, Ty21a, Quail, NVGH308 and LT2 strains) and in volunteer T5 and T6 PhoN), but could not be fully characterized in term of protein specificity, epitope mapping, haplotype restriction, and broad cross-reactivity. For the haplotype of volunteers used for the clonal analysis, and assays performed on the different volunteers see Supplementary Table 8.

Infection

Autologous EBV LCL were washed two time in RPMI 10% FCS in the absence of antibiotics, then plated at 10^6 per ml in the presence of different *Salmonella* strains at a multiplicity of infection between 90:1 and 10:1 varying from strain to strain to reach at least 30% of infected cells. After 2h of incubation, Gentamycin was added at 50ug/ml and cells were kept in culture overnight. Efficiency of infection was evaluated using anti-*Salmonella* CSA-1 antibody.

For the T cell macrophages transwell experiments Monocyte derived macrophages were differentiated for 5 days in the lower chamber of 24 well transwell plates (0.5×10^6 /well). At day 5 a pool of 3 CdtB specific clones for a total of 200000 cells/well was added to the upper well in the presence or absence of 5 μ g/ml CdtB peptide pool (CdtB). After O.N. incubation the upper well was removed, macrophages were washed, infected with *S. Typhimurium* (LT2 strain, Multiplicity of Infection=10) for 30m, washed again and incubated with Gentamicin (30mg/ml) to limit bacterial overgrowth.

Proteins

Proteins listed in Supplementary Table 2 were purified as His6 tagged proteins. Antigens were PCR-amplified from *Salmonella enterica* serovar Typhi Ty2 cloned into pET22b vector as previously described ²³. Antigens were expressed in *E.coli* BL21 and purified from inclusion bodies. Briefly, inclusion bodies (IB) were washed 3X in cold triton wash buffer (Tris-HCL 50mM, NaCl 100mM, DTT 1mM, EDTA 1mM, Triton X100 0.5%, Azide 0.1%) using glass homogenizer to remove bacterial debris and twice without triton, then solubilised in 8M urea solution (Tris-HCL 10mM, NaH₂PO₄ 100mM, DTT 0.1 mM, EDTA 0.1mM, Urea 8M). Further antigens were purified using Ni-NTA spin columns as per instructions (Qiagen, Cat.No. 31314) and stored at -80 in small aliquots.

HlyE and CdtB were PCR amplified from *Salmonella enterica* serovar Typhi Ty21a, cloned into pET21a vector and expressed in a LPS modified *E.coli* BL21 strain to produce endotoxin free proteins (Lucigen, ClearCoil BL21 cells). Soluble His-Tagged proteins were purified using HisTrap nickel affinity column (GE Healthcare) followed by desalting on a HiPrep 26/10 (GE Healthcare).

Peptide pools

Representative blocks of peptides overlapping by five amino acids were assembled for the proteins CdtB, HlyE and PhoN using BlockCons ³⁹ with sequences from distinct *S. Typhi*, *S. Paratyphi A* and *S. Typhimurium* strains (for peptide sequences, a list of bacterial strains and accession numbers see Supplementary Informations). Peptides were produced as Custom PEPscreen™ Peptide Libraries by Sigma.

Flow Cytometry

Whole blood was stained after ACK red blood cell lysis using a cocktail of antibodies directed against CD4 (OKT4, A700, Biolegend) CD8 (SK1, PerCPCy5.5, Biolegend), HLADR (L243, APC-Cy7, Biolegend), PD1 (eBioJ105, PE-eFluor610, eBioscience), CD3 (SK7, BV650, BD Bioscience), CD38 (HIT2, BB515, BD Bioscience), CD45RA (HT100, BV711, Biolegend), CCR7 (G043H7, PE-Cy7, Biolegend), Pan-TCRγδ (B1, BV421, Biolegend), Vα7.2(3C10, BV605, Biolegend), CD161 (HP-3G10, APC, eBioscience), αGalCer-CD1d-Tetramer (PE). Dead cells were excluded LIVE/DEAD® Fixable Aqua Dead Cell Stain Kit (Life Technologies Ltd). Samples were acquired on a BD LSRFortessa™ X20. For single cell FACS sorting, Whole blood was stained after ACK red blood cell lysis using a cocktail of antibodies directed against CD4 (OKT4, A700, Biolegend) CD8 (HIT8a,

PerCPCy5.5, Biolegend), CD3 (SK7, BV650, BD Bioscience), CD38 (HIT2, BB515, BD Bioscience), CCR7 (G043H7, PE/Cy7, Biolegend). Cell sorting was performed on BD FACS Aria™ Fusion Cell Sorter or BD FACS Aria™ III. Data was analyzed using FlowJo™ cell analysis software (FlowJo, LLC), Cytobank, and CyTOFkit.

HLADRB4*0101 class II tetramers loaded with peptide CdtB(105-125) SP110Y RYIYYSAIDVGARRVNLAIV, and with peptide ST CdtB (105-125) ST110H RYIYHSAIDVGARRVNLAIV, were produced by the Benaroya Tetramer core Facility. PBMC were thawed in presence of Benzonase and rested for 1h at 37C. 10⁶ PBMC were stained with 0.5µg of Tetramer in 50µl for 1h at RT. Dead cells were excluded with LIVE/DEAD® Fixable Aqua Dead Cell Stain Kit (Life Technologies Ltd), and cells were stained with CD4 (OKT4, A700, Biolegend) CD8 (HIT8a, PerCPCy5.5, Biolegend), CD14 (M5E2, Brilliant Violet 510™, Biolegend), CD19 (HIB19, BV510, Biolegend), CD38 (HIT2, BB515, BD Bioscience), CD45RA (HT100, BV711, Biolegend), CCR7 (G043H7, PE/Cy7, Biolegend). Samples were acquired on a BD LSRFortessa™.

TCR sequencing and analysis

RNA was extracted from individual clones or sorted cell populations using RNAqueous-Micro Total RNA Isolation Kit (Ambion), following the manufacturer's instructions. cDNA was generated by template switch reverse transcription using SMARTScribe Reverse Transcriptase (Clontech), using a template-switch oligo with a 6bp unique molecular identifier (TSO-UMI) and primers designed for the constant regions of Trac and Trbc genes. TCR amplification was achieved by performing two rounds of nested PCR using Phusion High-Fidelity PCR Master Mix (New England Biolabs). During the first PCR priming, indexes were included, to identify each sample. A last PCR was performed to add the Illumina adaptors. Primers' sequences are described in Supplementary Methods Table 4. TCR libraries were sequenced on Illumina Miseq using Miseq Reagent Kit V2 300-cycle (Illumina). FASTQ files were demultiplexed for each clone or cell population. Sequences from clones were analysed using MiXCR⁴⁰. Sequences from cell populations were analysed using MIGEC⁴¹. Post analysis was performed using VDJtools⁴².

Primer Sequences

Reverse transcription

TraRv0 5'-TCA GCT GGA CCA CAG CCG CAG-3'

TrbRv0 5'-CAG TAT CTG GAG TCA TTG A-3'

TSO-UMI 5'-CAG TGG TAT CAA CGC AGA GTA C NNN NNN rGrGrG-3' *

1st nested PCR

1stPCRFw-index 5'-CAC GAC GCT CTT CCG ATC TXX XXX XXX CAG TGG TAT CAA CGC AGA GTA C-3' **

1stPCRTraRv 5'-TAC ACG GCA GGG TCA GGG T-3'

1stPCRTrbRv 5'-TGC TTC TGA TGG CTC AAA CAC-3'

2nd nested PCR

2ndPCRFw 5'-CAC TCT TTC CCT ACA CGA CGC TCT TCC GAT C-3'

2ndPCRTraRv 5'-TGG AGT TCA GAC GTG TGC TCT TCC GAT CTG GGT CAG GGT TCT GGA TAT-3'

2ndPCRTrbRv 5'-TGG AGT TCA GAC GTG TGC TCT TCC GAT CTA CAC STT KTT CAG GTC CTC-3'

Illumina adaptors PCR

3rdPCRi7 5'-CAA GCA GAA GAC GGC ATA CGA GAT TCG CCT TAG TGA CTG GAG TTC AGA CGT G-3'

3rdPCRi5 5'-AAT GAT ACG GCG ACC ACC GAG ATC TAC ACC TCT CTA TAC ACT CTT TCC CTA CAC GAC-3'

* NNN NNN - unique molecular identifier

** XXX XXX - sample index

Statistical analysis

Statistical analysis was performed using Prism software (Graphpad). For multiple comparisons, either one-way analysis of variance (ANOVA) was used with Tukey's test to correct for multiple comparisons, or Friedman test with Dunn's test to correct for multiple comparisons. For comparison between two groups, either Student's paired two-tailed T test or Wilcoxon matched-pairs signed rank test, or One-tailed or Two-tailed Mann-Whitney test were used. Box extends from the 25th to the 75th percentile and whiskers from the minimum to the maximum value; line indicates median.

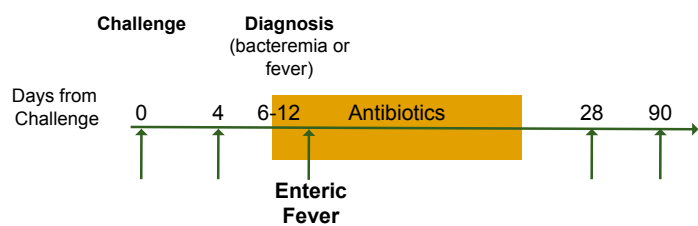
Material and Methods References

33. Dobinson, H.C. *et al.* Evaluation of the Clinical and Microbiological Response to Salmonella Paratyphi A Infection in the First Paratyphoid Human Challenge Model. *Clin Infect Dis* **64**, 1066-1073 (2017).

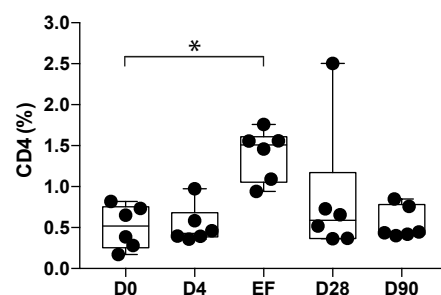
34. Wong, M.T. *et al.* Mapping the Diversity of Follicular Helper T Cells in Human Blood and Tonsils Using High-Dimensional Mass Cytometry Analysis. *Cell Rep* **11**, 1822-1833 (2015).
35. Finck, R. *et al.* Normalization of mass cytometry data with bead standards. *Cytometry A* **83**, 483-494 (2013).
36. Chen, H. *et al.* Cytofkit: A Bioconductor Package for an Integrated Mass Cytometry Data Analysis Pipeline. *PLoS Comput Biol* **12**, e1005112 (2016).
37. Kotecha, N., Krutzik, P.O. & Irish, J.M. Web-based analysis and publication of flow cytometry experiments. *Curr Protoc Cytom* **Chapter 10**, Unit10 17 (2010).
38. Traunecker, A., Oliveri, F. & Karjalainen, K. Myeloma based expression system for production of large mammalian proteins. *Trends Biotechnol* **9**, 109-113 (1991).
39. Olsen, L.R. *et al.* BlockLogo: visualization of peptide and sequence motif conservation. *J Immunol Methods* **400-401**, 37-44 (2013).
40. Bolotin, D.A. *et al.* MiXCR: software for comprehensive adaptive immunity profiling. *Nat Methods* **12**, 380-381 (2015).
41. Shugay, M. *et al.* Towards error-free profiling of immune repertoires. *Nat Methods* **11**, 653-655 (2014).
42. Shugay, M. *et al.* VDJtools: Unifying Post-analysis of T Cell Receptor Repertoires. *PLoS Comput Biol* **11**, e1004503 (2015).

Figure 1

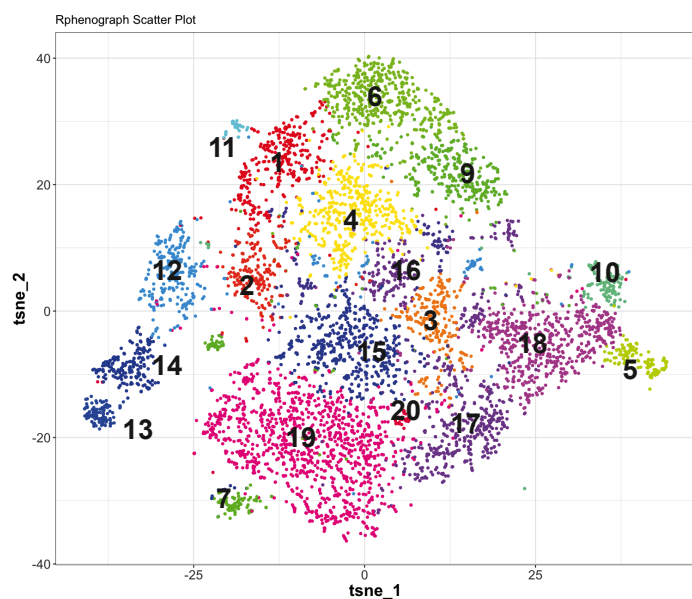
a



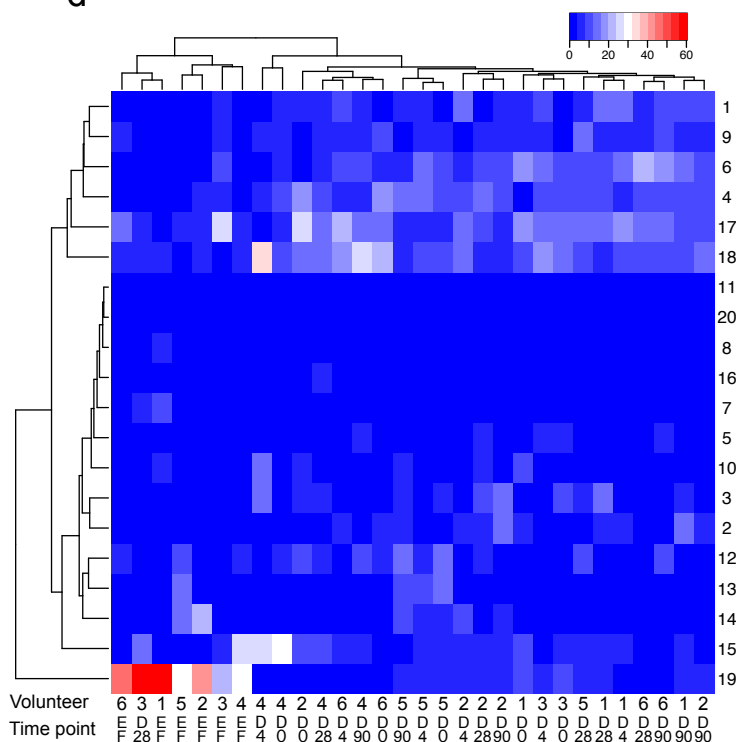
b



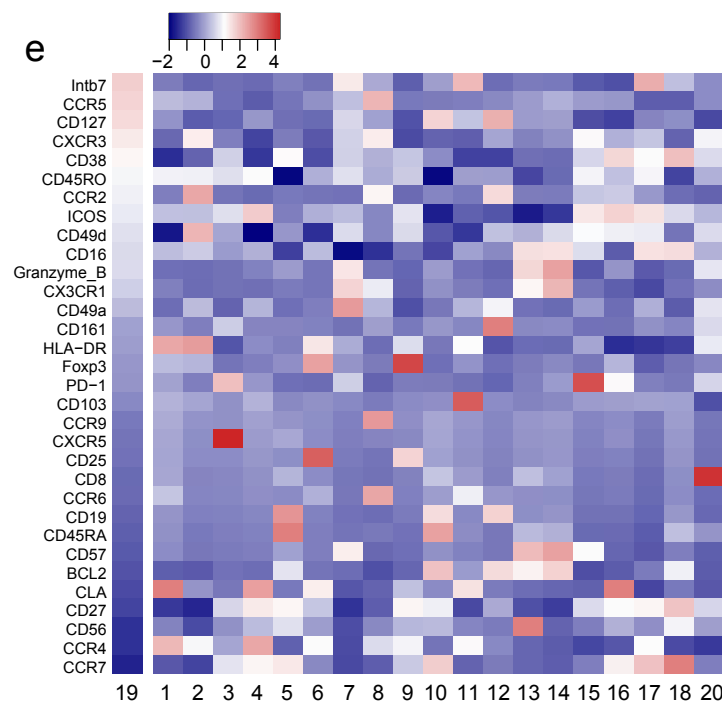
C



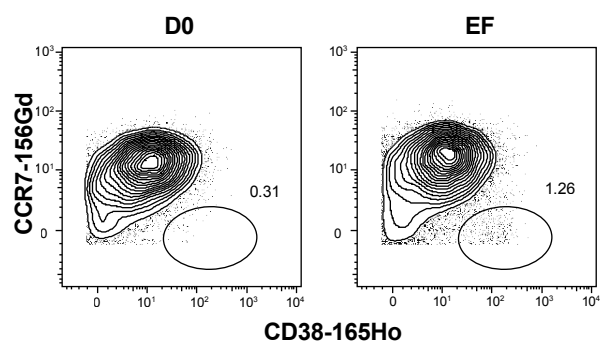
d



e



f



g

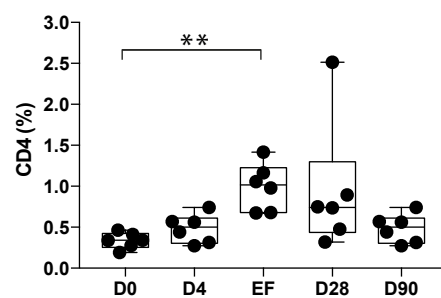


Figure 2

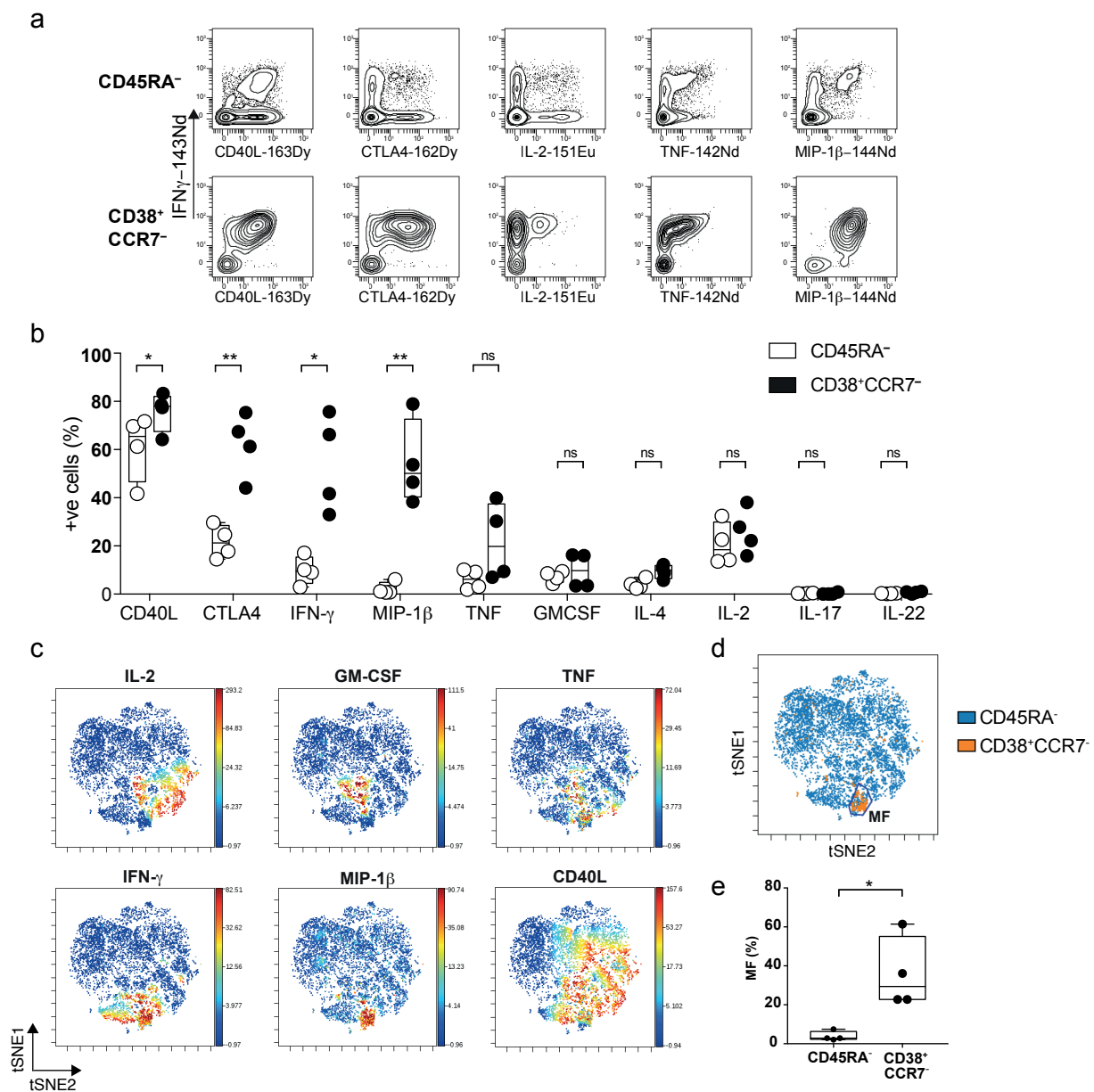


Figure 3

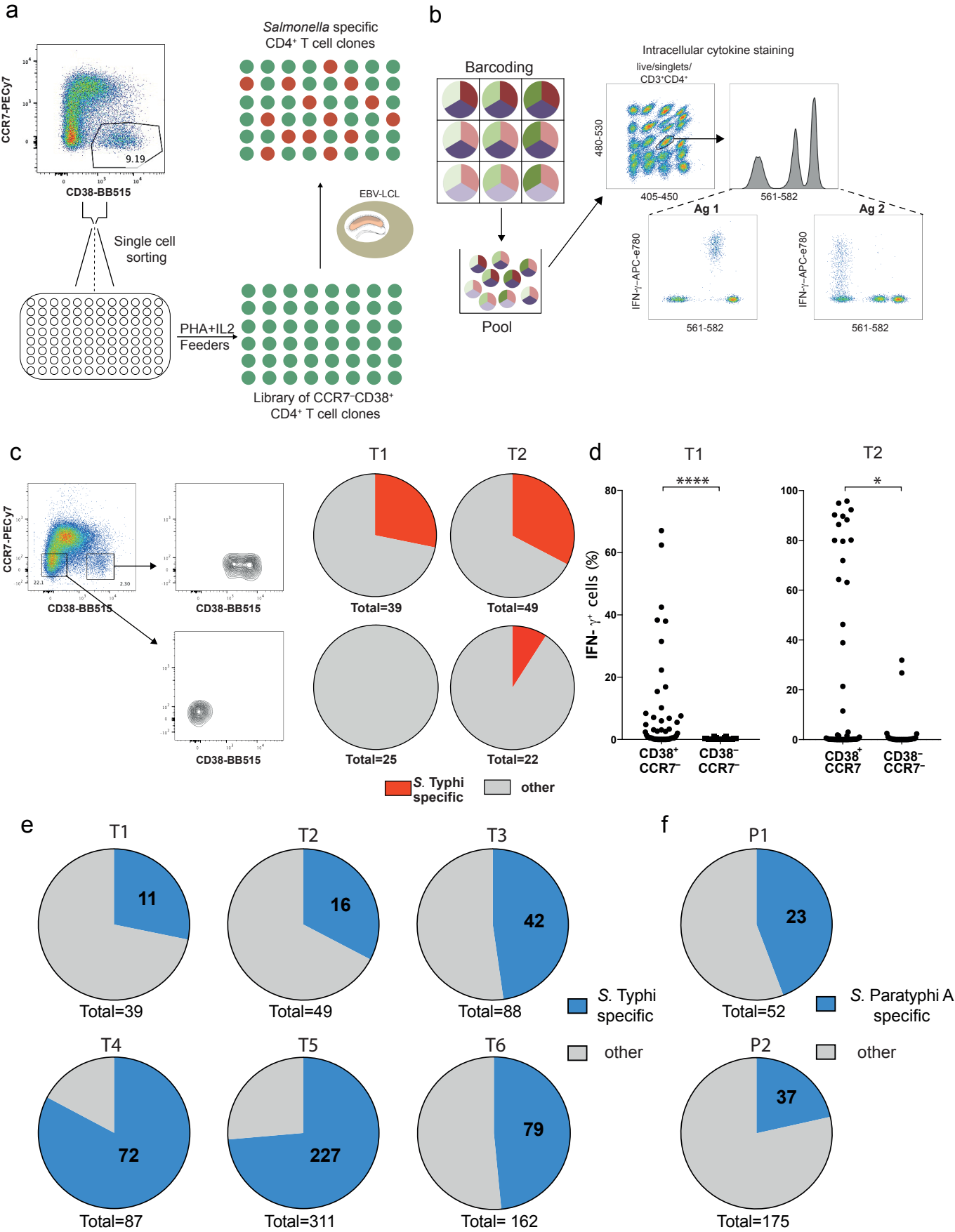


Figure 4

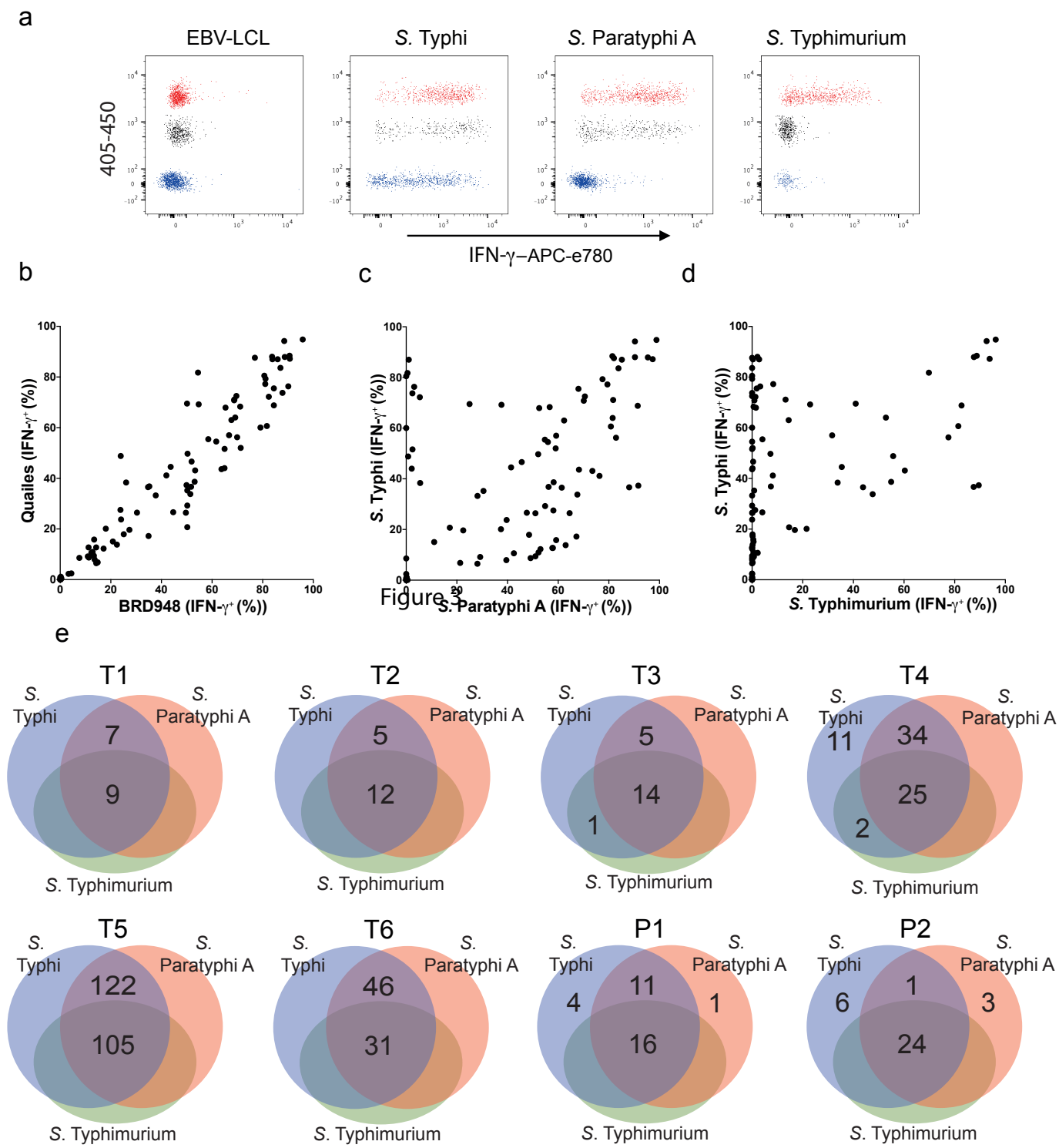


Figure 5

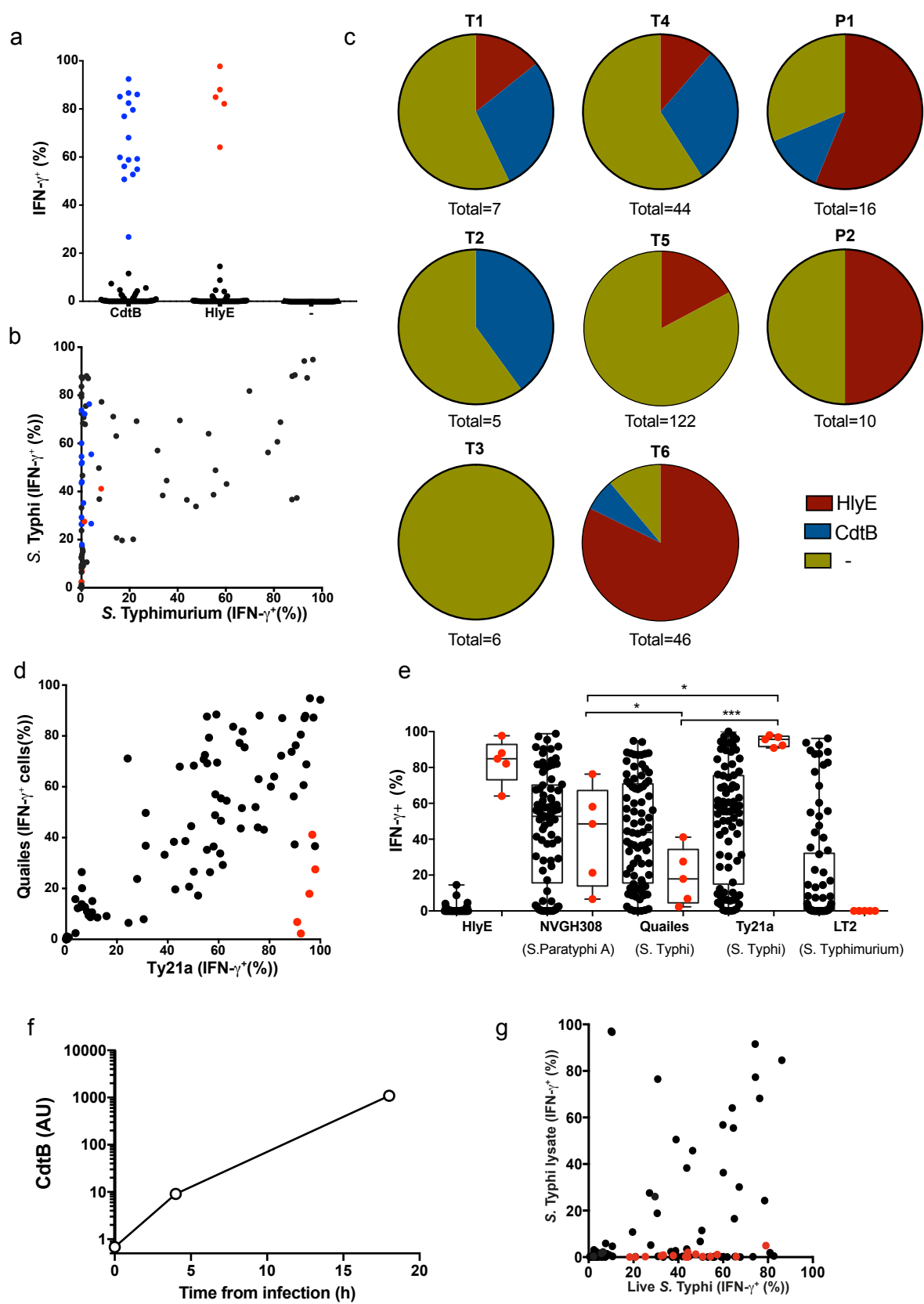


Figure 6

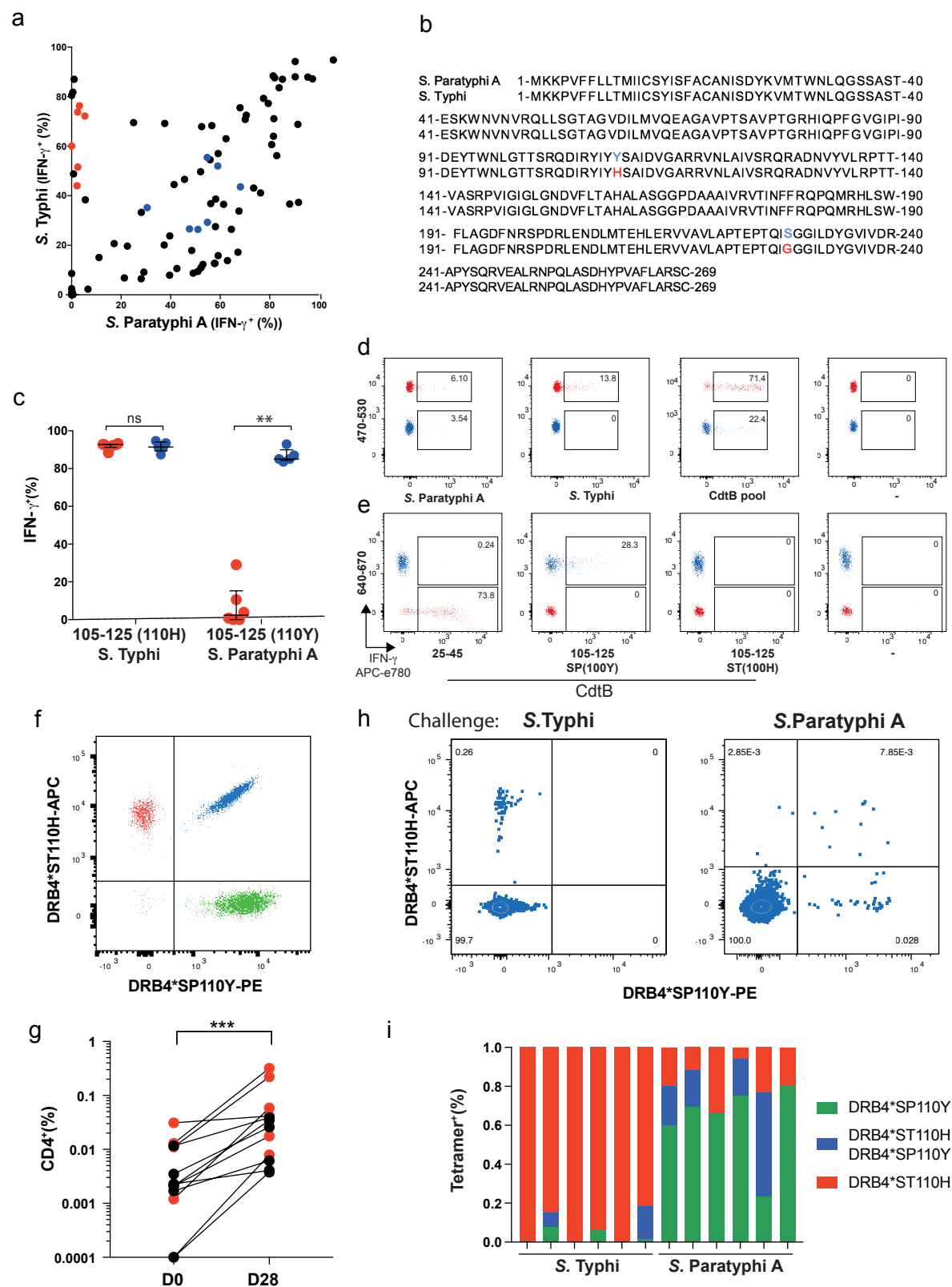


Figure 7

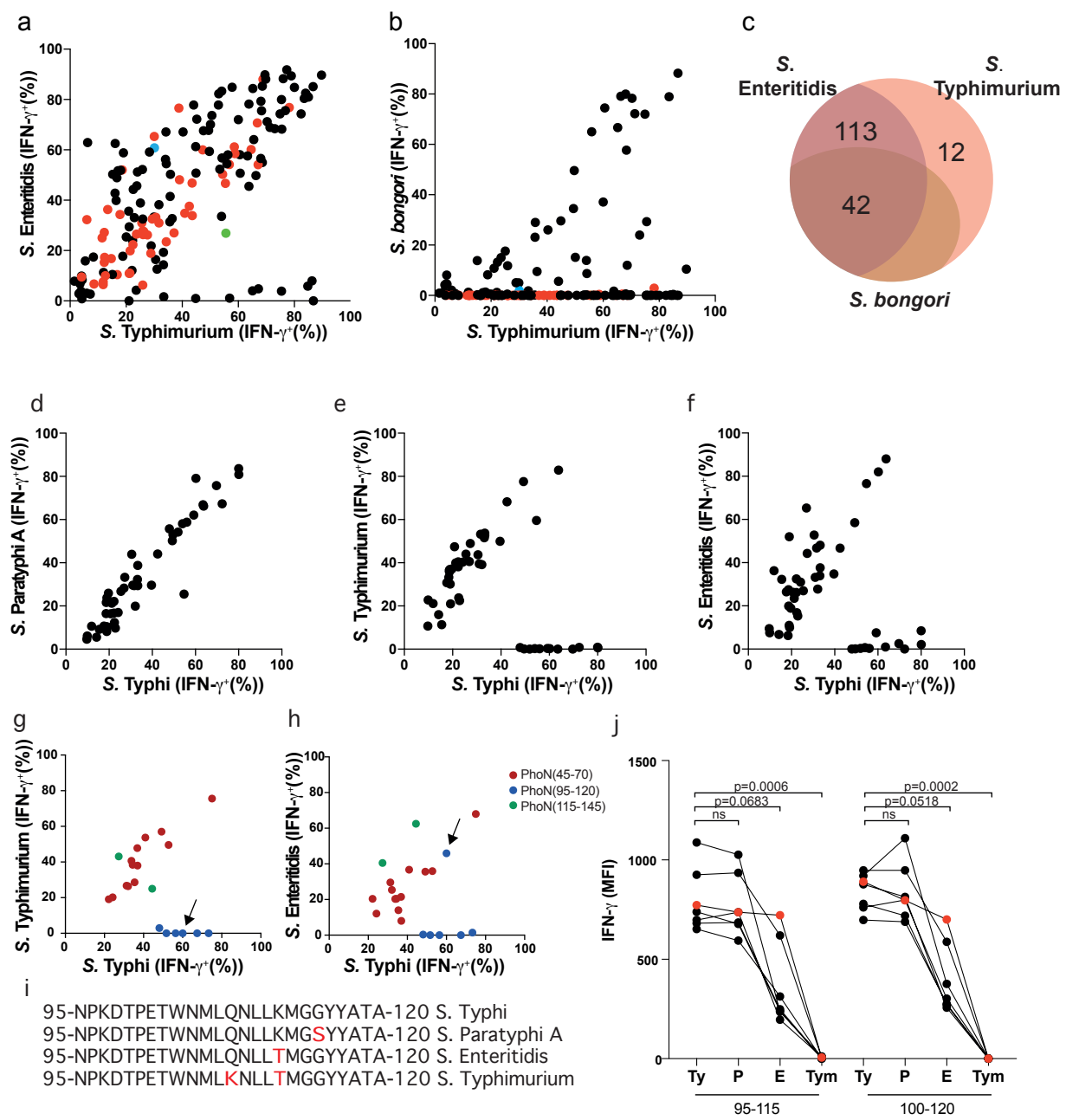
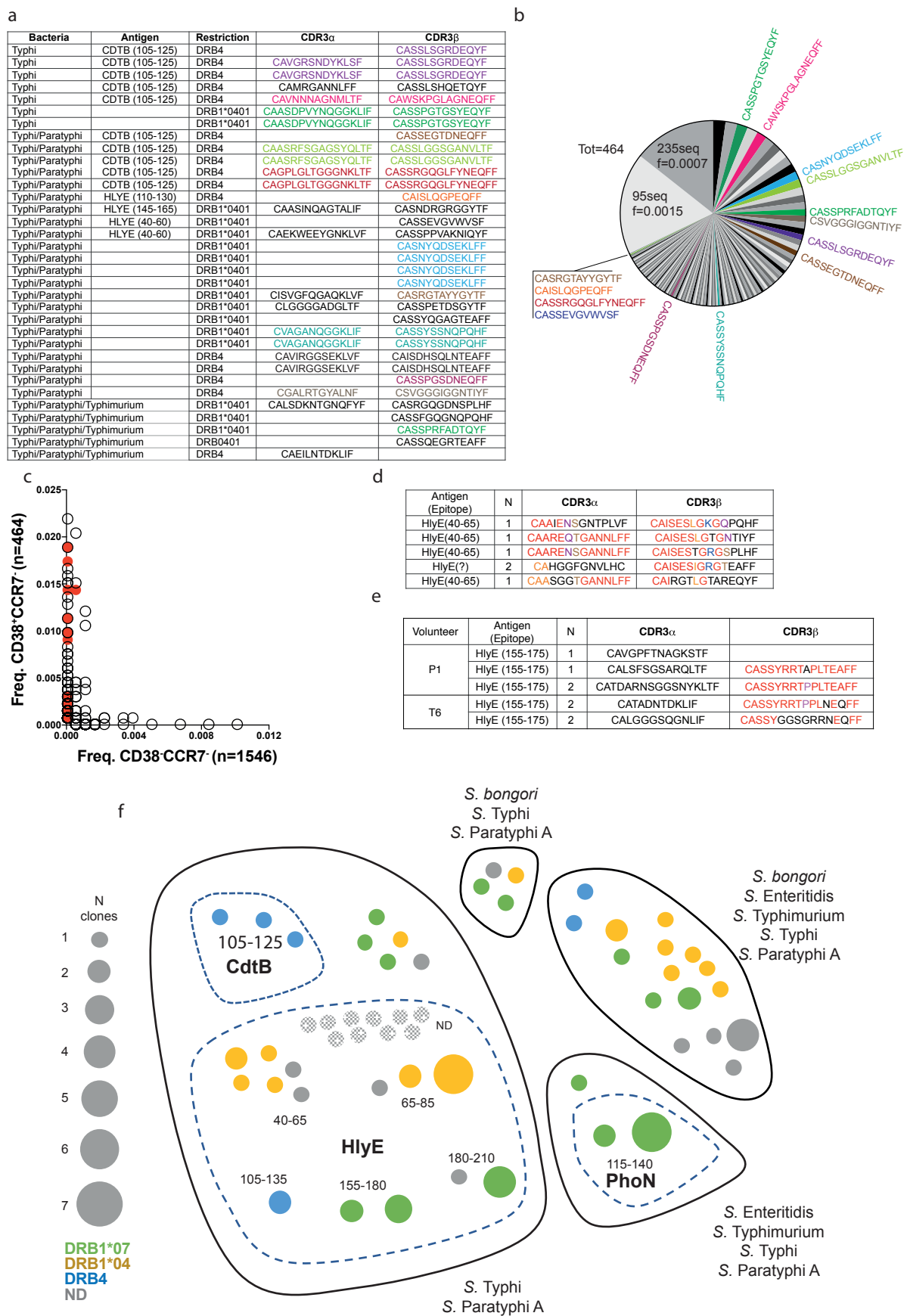
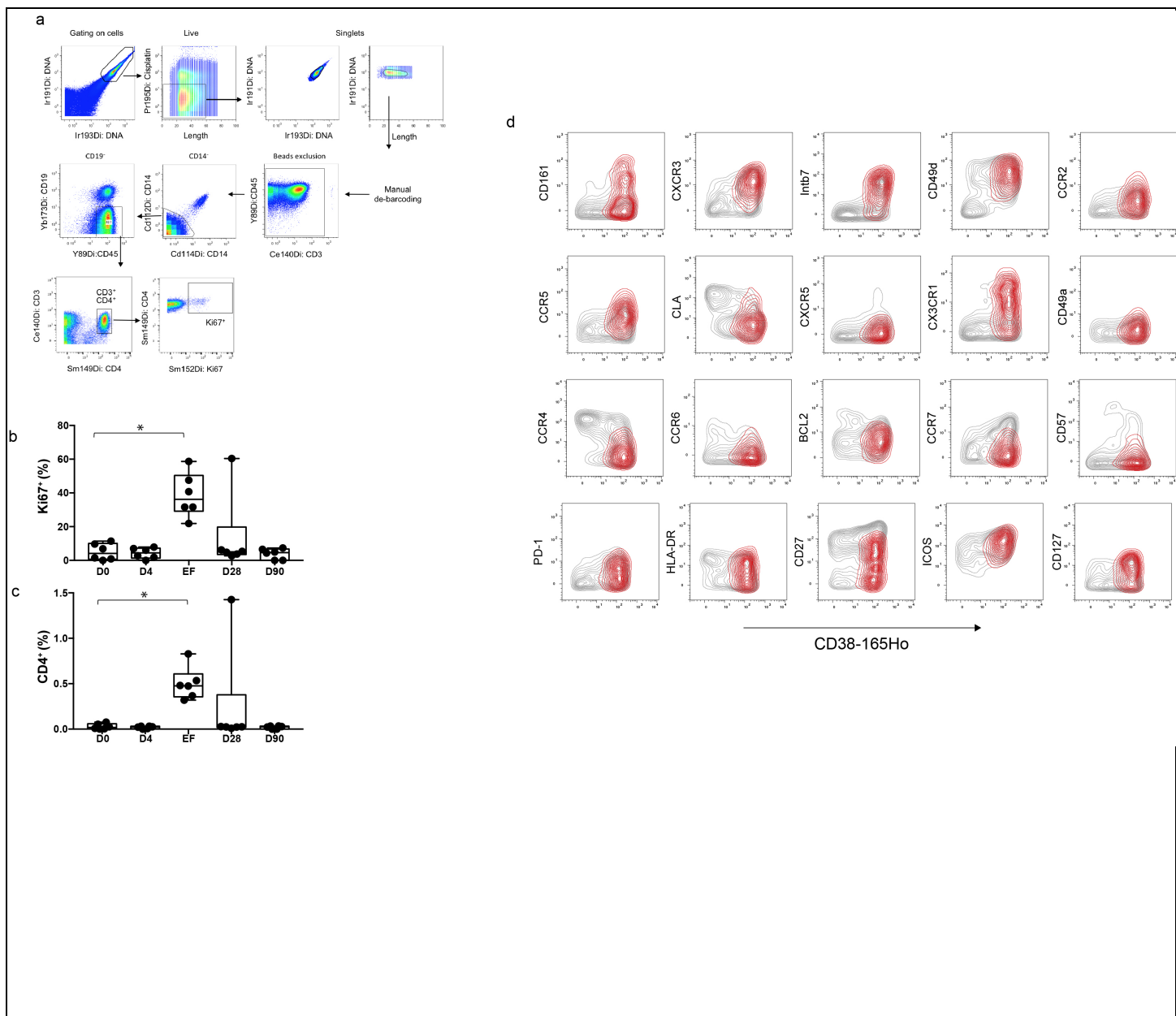


Figure 8

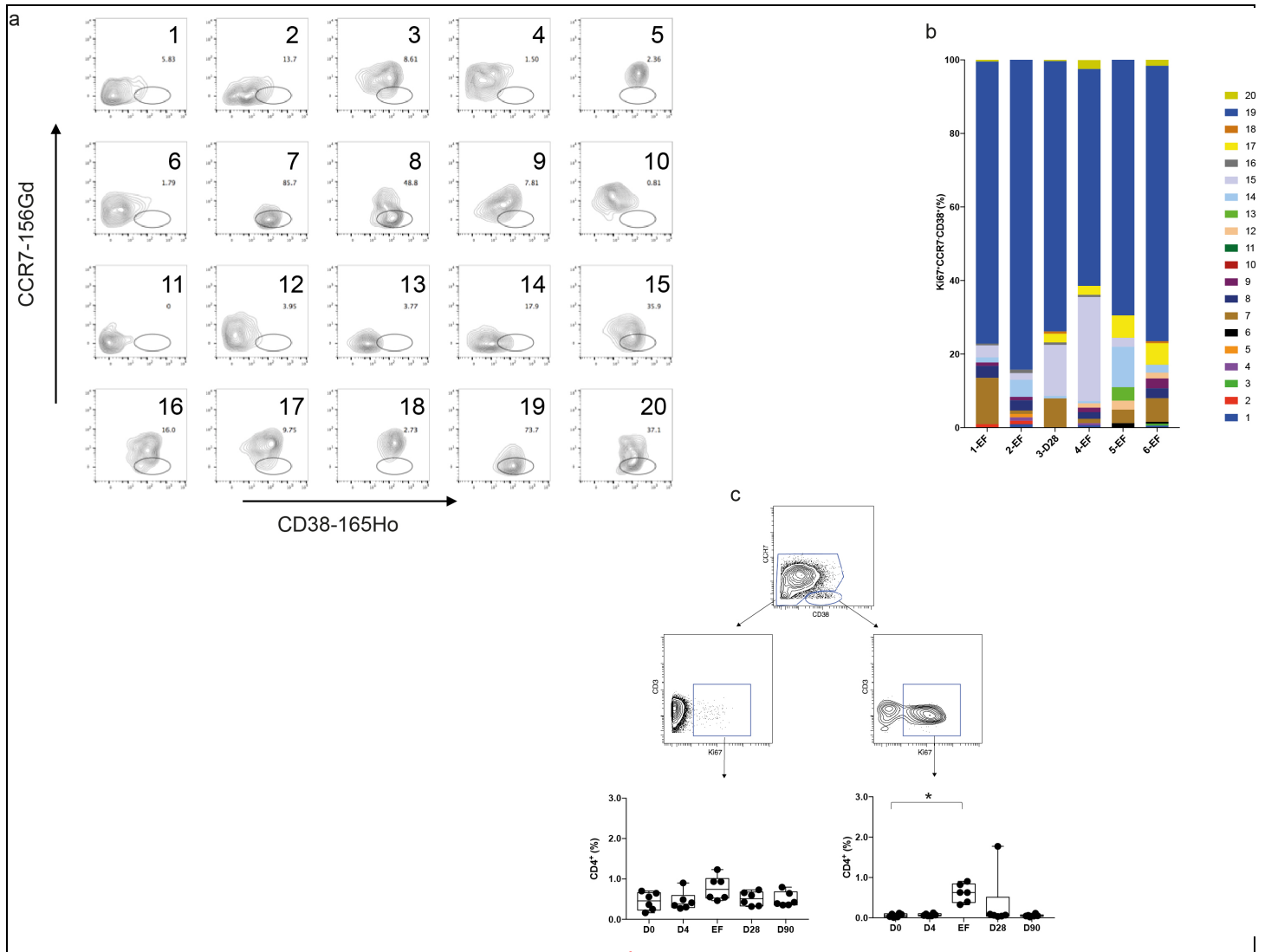




Supplementary Figure 1

Characterization of Ki67⁺ cells accumulating during enteric fever

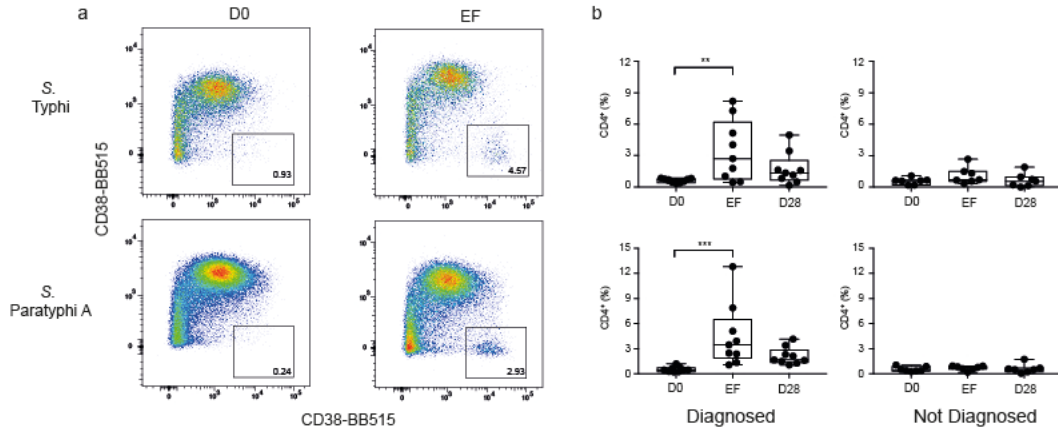
(a) Gating strategy to identify CD4⁺ and CD4⁺Ki67⁺ cells in Mass Cytometry experiments. Frequency of Cluster 19 cells within Ki67⁺ **(b)** and total CD4⁺ T cells **(c)** at different time points after infection (n=6). **(b)** Friedman Test p=0.0147, Dunn's Multiple Comparison Test D0 vs D4, D28, D90 p=ns, D0 vs EF p= 0.027. **(c)** Friedman Test p=0.0159, Dunn's Multiple Comparison Test D0 vs D4, D28, D90 p=ns, D0 vs EF p=0.0247. **(d)** Total Ki67⁺ events (grey) and Cluster 19 events (red) across all samples were concatenated and expression of 20 markers against CD38 in the distinct populations is shown.



Supplementary Figure 2

CCR7⁺CD38⁺CD4⁺ cells are enriched in Ki67⁺ accumulating during enteric fever

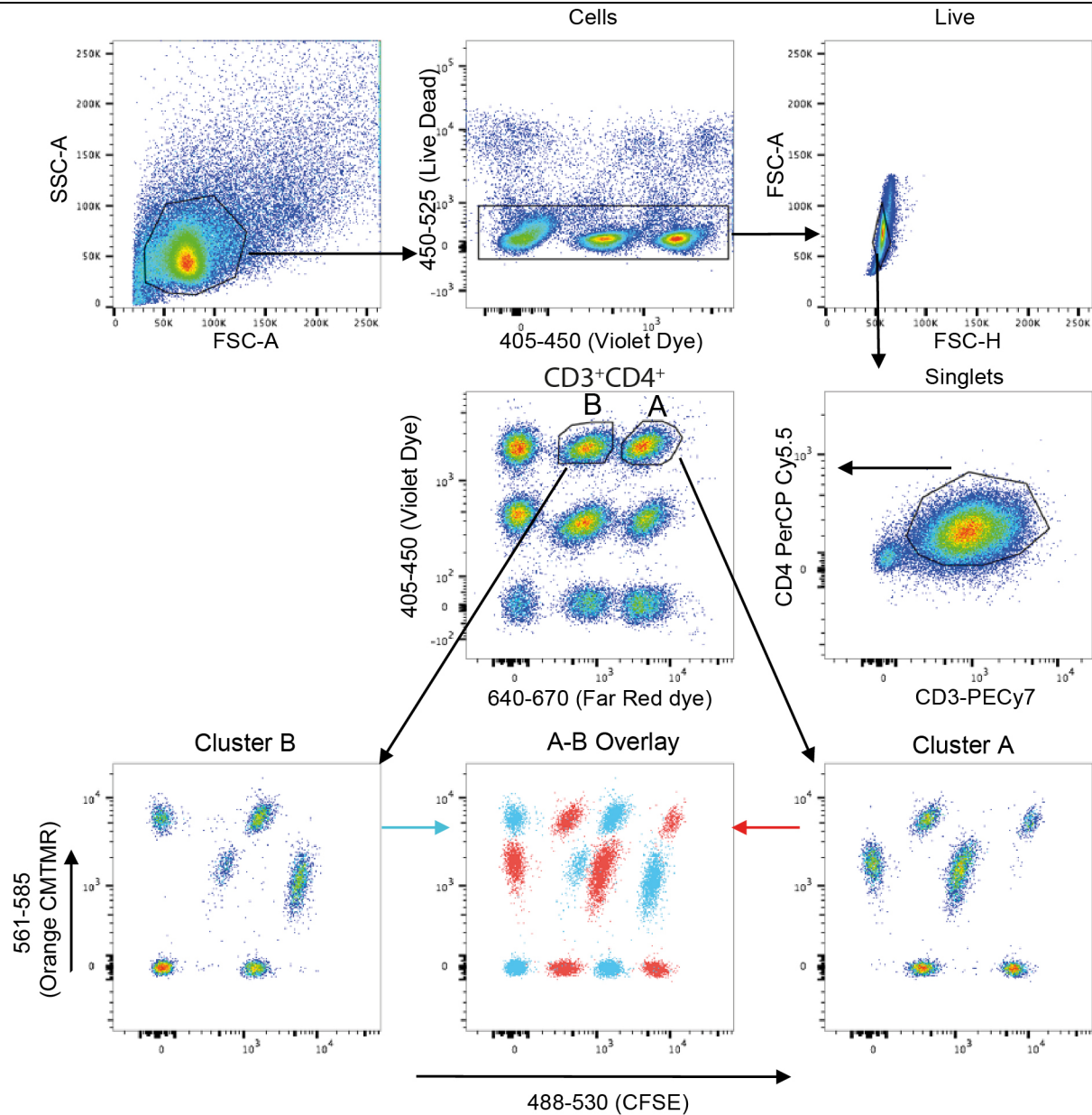
(a) Expression of CCR7 and CD38 in the 20 distinct clusters identified by PhenoGraph analysis. (b) Proportion of PhenoGraph clusters within Ki67⁺ CD38⁺CCR7⁻ cells at the peak of Ki67⁺ cell accumulation. (c) Frequency of Ki67⁺ CD38⁺CCR7⁻ cells (Friedman Test $p=0.0130$, Dunn's Multiple Comparison Test D0 vs D4, D28, D90 $p=ns$, D0 vs EF $p=0.0139$) and of Ki67⁺ cells non comprised within CD38⁺CCR7⁻ cells over time in challenged volunteers ($n=6$) (Friedman Test $p=0.23$, Dunn's Multiple Comparison Test D0 vs D4, EF, D28, D90 $p=ns$). Box extends from the 25th to the 75th percentile and whiskers from the minimum to the maximum value; line indicates median.



Supplementary Figure 3

Accumulation of CD4⁺CD38⁺CCR7⁻ in whole blood of volunteers with enteric fever.

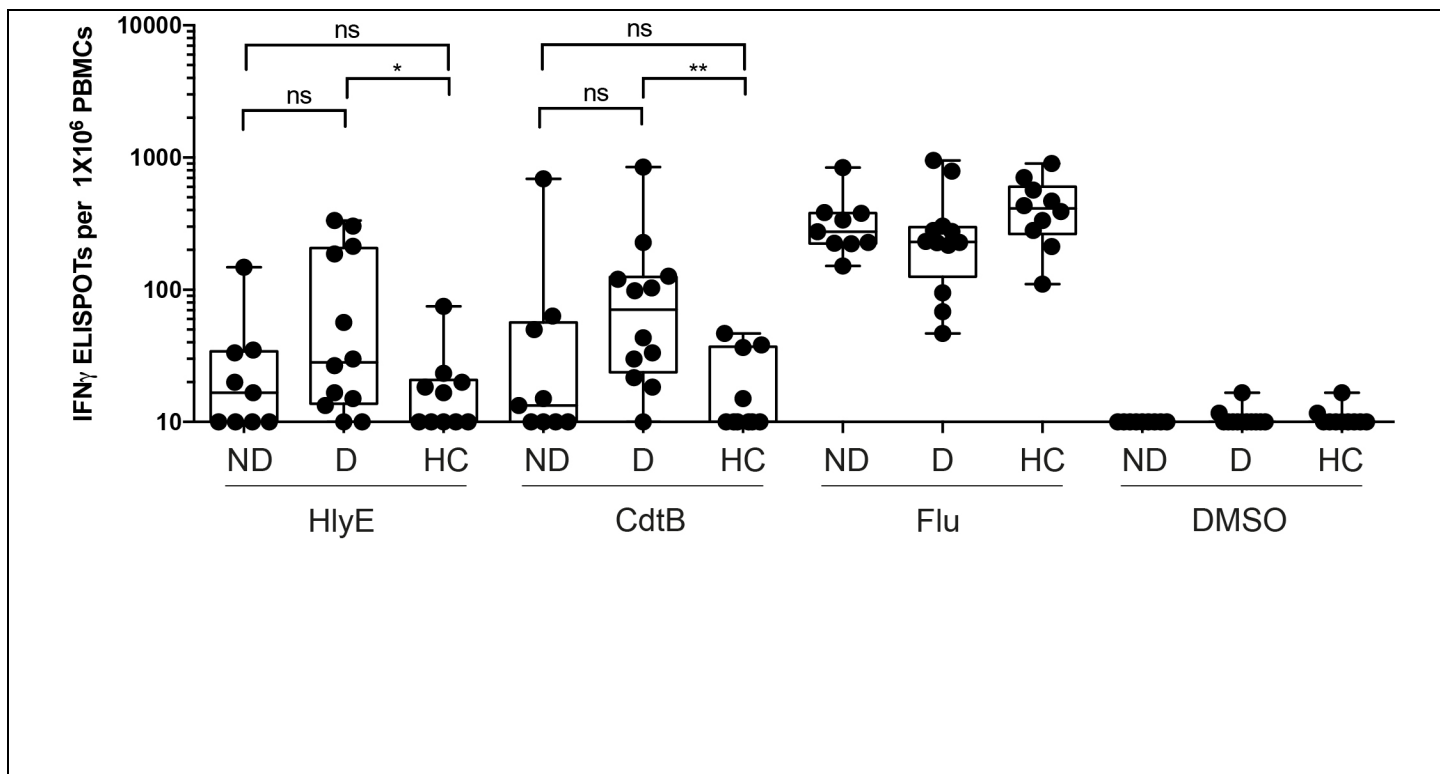
(a) Identification of CD4⁺CD38⁺CCR7⁻ cells during enteric fever by Multicolour Flow Cytometry in whole blood from a representative volunteer challenged with *S. Typhi*, and one challenged with *S. Paratyphi A*. **(b)** Accumulation of CD38⁺CCR7⁻ cells after diagnosis in volunteers challenged with *S. Typhi* and *Paratyphi A* who developed (Diagnosed) but not in those who did not develop enteric fever (Not Diagnosed). In challenged volunteers not diagnosed blood was collected 14 days after challenge (D14). Friedman Multi comparison Test $p=0.006$ (*S. Typhi*), $p<0.0001$ (*S. Paratyphi*). Dunn's Multiple Comparison Test ED vs D0, $p=0.0065$ (*Typhi*, $n=9$); $p=0.0002$ (*S. Paratyphi A*, $n=9$). Box extends from the 25th to the 75th percentile and whiskers from the minimum to the maximum value; line indicates median.



Supplementary Figure 4

Gating strategy for live fluorescent barcoding of T cell clones

Shown is an example with four live fluorescent dyes. Cells were labelled with 9 combinations of three distinct dilutions of Violet and Far red dyes. Cells with each of the nine clusters were labelled with 6 combinations of 4 distinct dilutions of CFSE and 3 of CMTMR orange dyes. Dilutions used for adjacent clusters across the 640-670 axis were labelled with alternate dilutions of CFSE and CMTMR Orange (as shown in the overlaid plots) in order to reduce spill-over in case of suboptimal separation between clusters across the channel-dye combination with the lowest stain index.

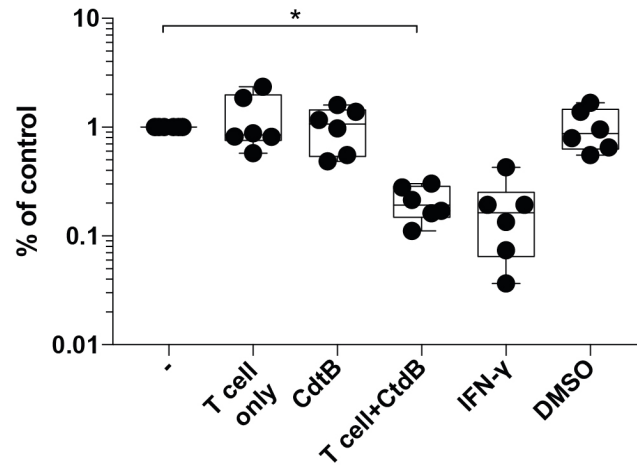


Supplementary Figure 5

Increased frequency of HlyE and CdtB specific T cells in volunteers diagnosed with enteric fever.

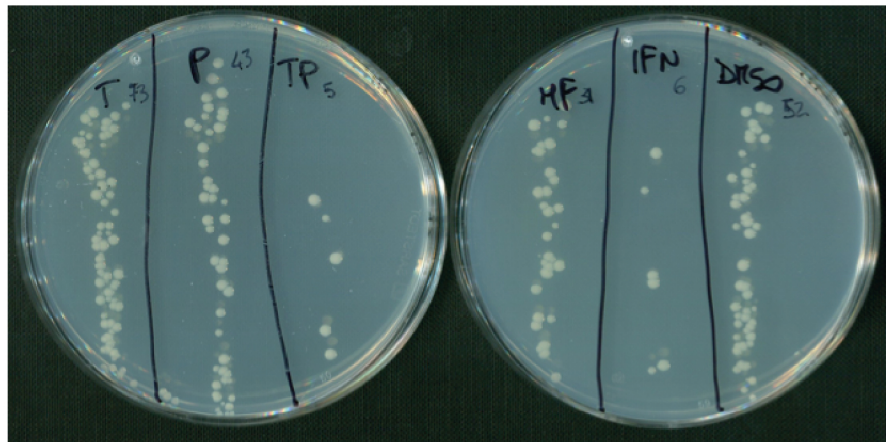
(a) Frequency of HlyE, CdtB and Flu specific T cell responses 28 days after challenge measured by IFN- γ ELISPOT in volunteers challenged with *S. Typhi* or *S. Paratyphi A* who developed (Diagnosed, D, $n=12$) or did not develop (Not Diagnosed, ND, $n=9$) enteric fever compared to uninfected controls (HC, $n=10$). Freshly isolated PBMC were rested overnight and incubated with $5 \mu\text{g/ml}$ of HlyE or CdtB peptide pools, or with inactivated seasonal influenza vaccine (Flu). Mann Whitney two tailed t-test. $*$ = $p<0.05$; $**$ = $p<0.005$. Box extends from the 25th to the 75th percentile and whiskers from the minimum to the maximum value; line indicates median.

a



b

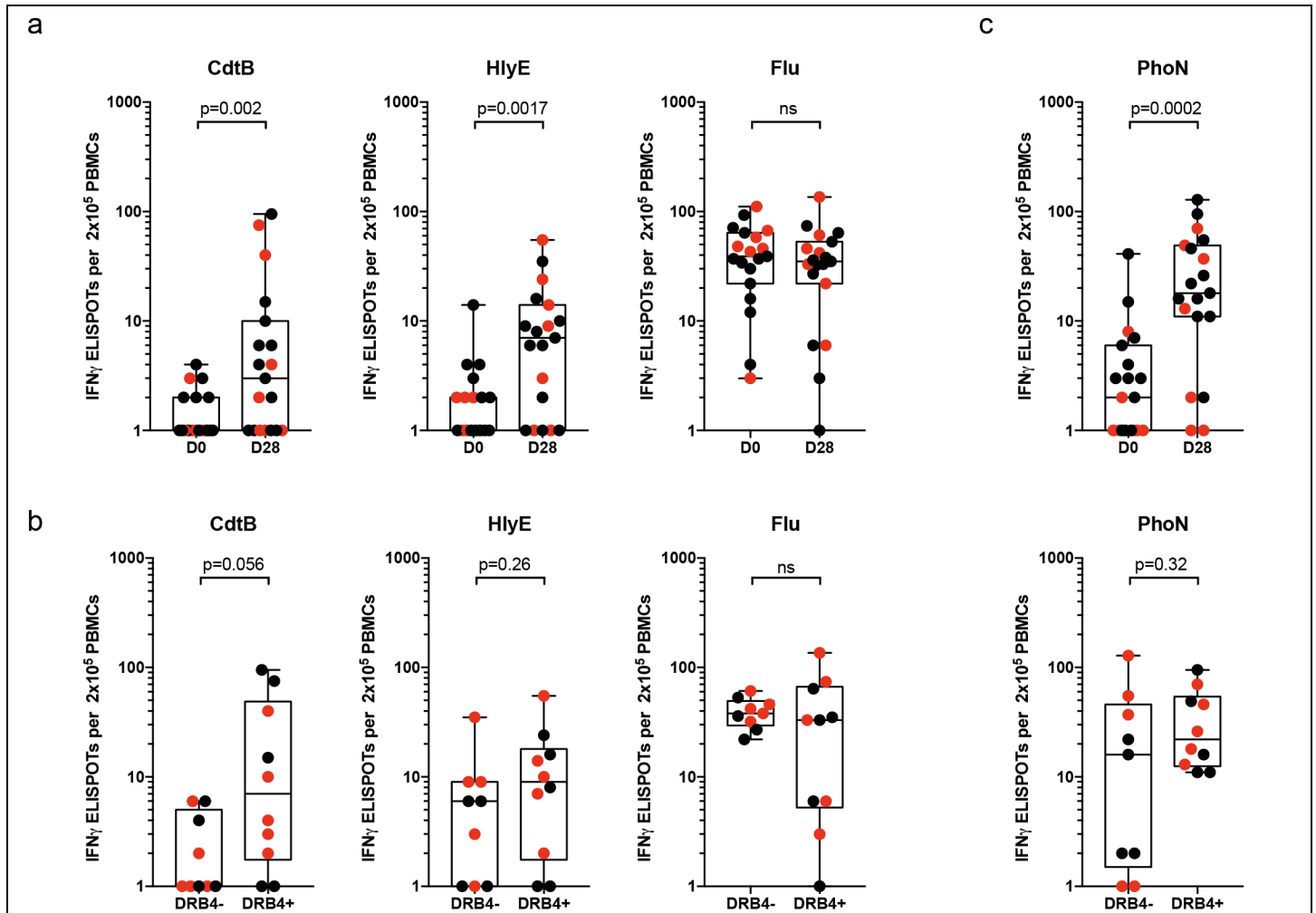
T cells only CdtB pool T cells + CdtB pool MF only IFN-γ DMSO



Supplementary Figure 6

CdtB specific clones help macrophages to limit bacterial spread.

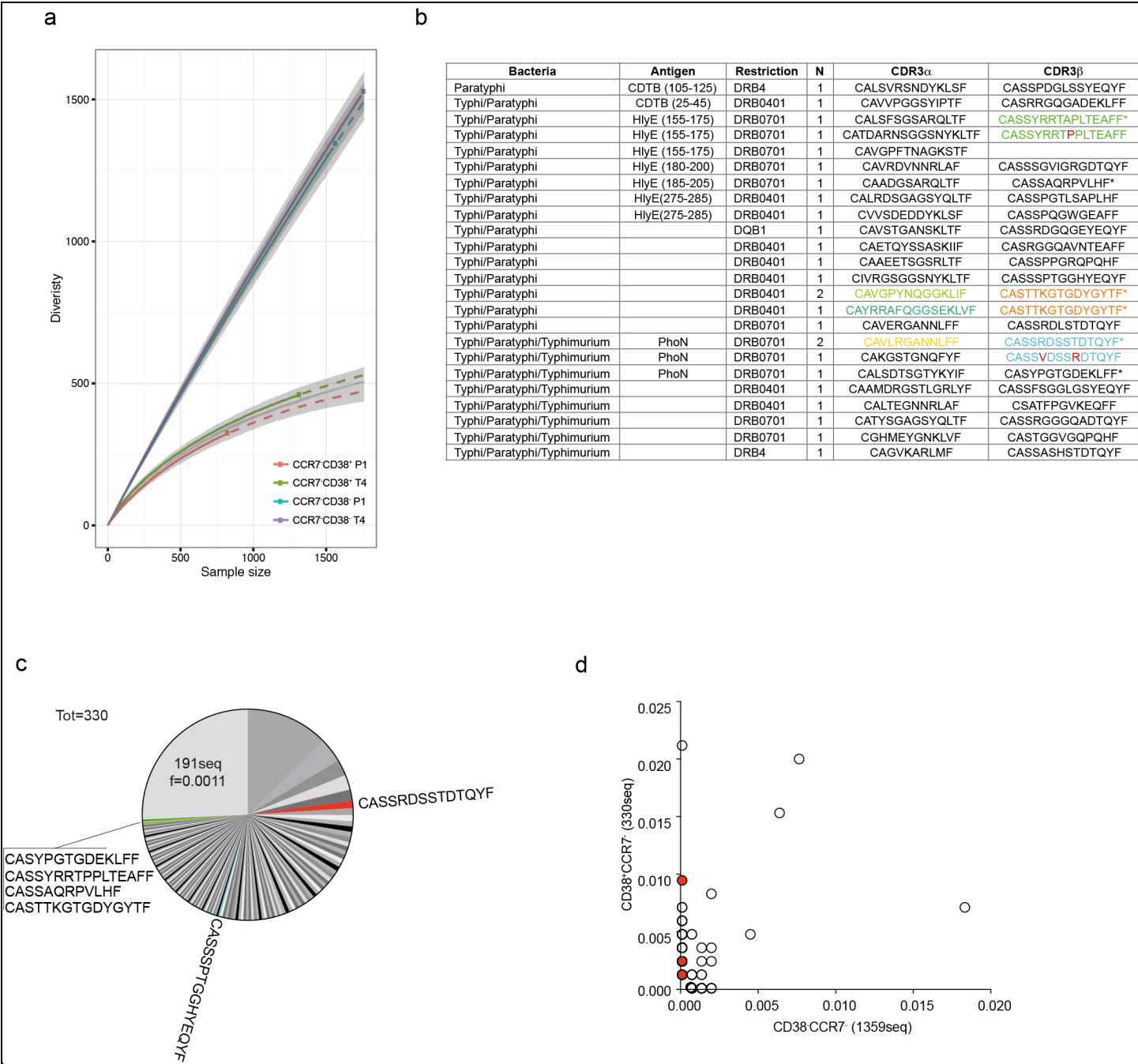
(a) Monocyte derived macrophages (MF) were differentiated for 5 days in the lower chamber of 24 well transwell plates. At day 5 a pool of 3 CdtB specific clones (T) was added to the upper well in the presence or absence of CdtB peptide pool (CdtB). After O.N. incubation, upper well was removed, macrophages were washed, infected with *S. Typhimurium* (LT2 strain) for 30m, washed again and incubated with Gentamicin (30mg/ml) to limit bacterial overgrowth. 2h after infection cell culture supernatant was plated in agar plates and colonies counted after over night culture. Indicated is the percentage of bacterial growth compared to macrophages alone (n=6, Friedman test (p=0.0008) with Dunn's multiple comparisons test (control vs T+CdtB p=0.0169). Box extends from the 25th to the 75th percentile and whiskers from the minimum to the maximum value; line indicates median. (b) CFU after O.N. culture of macrophage supernatant in agar plate in one representative experiment.



Supplementary Figure 7

Increased Frequency of CdtB, HlyE and PhoN T cell responses after diagnosis of Enteric Fever.

(a) Frequency of HlyE, CdtB, and Flu specific T cell responses at baseline and 28 days after challenge measured by IFN-g ELISPOT in frozen PBMC from volunteers challenged with *S. Typhi* or *S. Paratyphi A* who developed ($n=19$) enteric fever (Wilcoxon matched-pairs signed rank test). **(b)** Frequency of HlyE, CdtB, PhoN and Flu specific T cell responses in HLADRB4+ and HLADRB4- volunteers 28 days after challenge (Mann Whitney test two-tailed p value). **(c)** Frequency of PhoN specific T cell responses at baseline and 28 days after challenge measured by IFN-g ELISPOT in frozen PBMC from volunteers challenged with *S. Typhi* or *S. Paratyphi A* who developed ($n=19$) enteric fever and in HLADRB4+ and HLADRB4- individuals. ELISPOT analysis done on the same frozen samples as in panel **a** and **b**.



Supplementary Figure 6

Clonal expansion of Salmonella specific effector T cells.

(a) Rarefaction curve describing the estimated diversity of the CDR3β repertoire of CD38⁺CCR7⁻ and CD38⁻CCR7⁻ subsets in volunteers P1 and T4. Dots between continuous and dashed curves indicate the number of TCRs identified within each sample. Number of cells probed: P1 CD38⁺CCR7⁻ =5087 cells, CD38⁻CCR7⁻ = 1.15e10⁵ cells; T4 CD38⁺CCR7⁻ =9130 cells, CD38⁻CCR7⁻ = 1.3e10⁵ cells. (b) Pathogen selectivity, antigen specificity, restriction, CDR3α and CDR3β sequence of clones isolated from volunteer P1. Starred(*) sequences were identified also in the polyclonal analysis. (c) Pie Chart depicting the frequency of CDR3β sequences within the polyclonal repertoire of CD38⁺CCR7⁻ cells (5087 cells probed) from T4, highlighted are the CDR3β sequences identified in the isolated clones. (d)

Frequency of CDR3 β within the polyclonal repertoire of CD38⁺CCR7⁻ cells and CD38⁻CCR7⁻ cells in volunteer P1 (1.15e10⁵ cells probed).
Red circles represent CDR3 β sequences identified in the isolated clones.